

Fermi National Accelerator Laboratory

**FN-477-Rev.
[SSC-163]**

Resonant Impedance in a Toroidal Beam Pipe*

King-Yuen Ng
SSC Central Design Group
c/o Lawrence Berkeley Laboratory 90/4040
Berkeley, California 94720
and
Fermi National Accelerator Laboratory
P.O. Box 500, Batavia, Illinois

Revised May 1988

Submitted to Part. Accel.



Operated by Universities Research Association Inc. under contract with the United States Department of Energy

SSC-163
FN-477

RESONANT IMPEDANCE IN A TOROIDAL BEAM PIPE

King-Yuen Ng

SSC Central Design Group*

c/o Lawrence Berkeley Laboratory 90/4040, Berkeley, CA 94720

and

Fermi National Accelerator Laboratory*

Batavia, IL 60510

(February 1988)

(Revised May 1988)

Submitted to Particle Accelerators

ABSTRACT

The electromagnetic fields generated by a beam inside a toroidal beam pipe are derived. Special attention has been given to the resonances developed. The effective impedance seen by the beam is computed and the effects of displacing the beam away the beam pipe center are considered. Applications are made to the SSC and the TEVATRON.

*Operated by the Universities Research Association, Inc., under contracts with the U.S. Department of Energy.

I. INTRODUCTION

All electromagnetic waves that can propagate in a *straight* beam pipe must have phase velocities larger than c , the velocity of light. As a result, the particle beam can never catch up with them and no resonance can occur, because the wave traveling with it will never have a velocity exceeding c . The situation of a *curved* toroidal beam pipe is quite different. The wave with a particular azimuthal harmonic n travels with different *linear* phase velocities depending on the distance from the center of the toroidal ring. For example, if the beam travels with velocity βc at a toroidal radius R , the electromagnetic wave traveling with the beam will have a phase velocity $r\beta c/R$ at a radius r . When this phase velocity exceeds c , the electromagnetic wave should be able to propagate, in analogy to the *straight* beam pipe. The condition for this to happen is therefore

$$\frac{R_+\beta}{R} > 1, \quad (1.1)$$

where R_+ is the radius of the outer edge of the beam pipe. Under this situation, the electromagnetic wave generated by the beam interacts with the beam. In other words, a resonance occurs and the beam sees an impedance. This problem has been studied by Laslett-Lewish¹ and Faltens-Laslett.² Our approach, way of solution, and interpretation on the impedance seen are different from theirs. Our first attack on this problem was done in 1980 when longitudinal coupling impedance for the Energy-Doubler (or the TEVATRON) was examined,³ but no detailed report was written at that time.

The main concern here is the SSC. We want to investigate whether these resonances will affect the stability of the beam. The SSC main ring has a mean ring radius of 13200.95 m and a beam pipe radius of $b = 1.5$ cm. If the beam is at the center of the beam pipe, resonance can occur when the relativistic $\gamma > 663$ according to criterion (1.1). Therefore we expect the beam to meet these resonances for the whole acceleration and storage cycle.

For a wave that can ‘propagate’ inside a beam pipe of cross-sectional size b , the wavelength must be less than or of the order of b or the azimuthal harmonic must be bigger than the cutoff harmonic given by

$$n_{co} = O\left(\frac{R}{b}\right), \quad (1.2)$$

where $2\pi R$ is the length of the particle orbit. For the toroidal beam pipe, in order that the particle beam can catch up with the resonant wave, the condition is more restrictive, because boundary conditions have to be met in all three directions. The propagating electromagnetic wave, which has to travel with velocity c or bigger, is

confined mainly to a small region near the outer edge of the beam pipe. Therefore, the wavelength will be much less than b . As it turns out in Section III, these resonant waves have a lowest azimuthal harmonic n_{11} given by

$$n_{11} = O\left(n_{co}^{3/2}\right) . \quad (1.3)$$

For a machine such as the SSC which has a large ring radius and a very narrow beam pipe radius, the cutoff harmonic $n_{co} = 2.12 \times 10^6$ is very big. Thus the lowest resonant toroidal harmonic $n_{11} \sim O(10^9)$ is very much larger than n_{co} . The effective impedance per unit harmonic of this lowest mode seen by the beam turns out to be 0.36Ω at ~ 20 TeV. But the SSC bunch has a rms length of $\sigma_t = 7$ cm or a spectrum extending to a rms harmonic of only 1.89×10^5 . Therefore these toroidal resonances should have negligible effect on the single bunch mode stability. This impedance can still drive a microwave growth, however. But this growth will be damped completely by the designed momentum spread of the beam. On the other hand, the story can be quite different for a small storage ring with a large beam pipe radius, because n_{co} will be small and the lowest toroidal resonant harmonics may not be larger than n_{co} by very much.

In Section II, the fields excited by the particle beam in the toroidal beam pipe are computed by assuming perfectly conducting pipe wall. In Section III, we pick out the resonances and compute the resonant harmonics. The SSC main ring is used as an example. The figures of merit Q and the shunt impedances Z_{sh} of some lower resonant modes are derived in Section IV using the usual perturbative method by the introduction of a finite wall conductivity. In Section V, the effective impedance seen by the beam is computed. Finally in Section VI, the application is extended to the SSC booster rings and the TEVATRON.

II. THE FIELDS IN A TOROIDAL BEAM PIPE

II.1 The model

We shall use the Gaussian units except when specified otherwise. To simplify the mathematics, we consider a toroidal beam pipe with a rectangular cross section: width $2b$ and height h as shown in Fig. 1. Consider a beam in the mid-plane at a radius R , having a single azimuthal harmonic n , traveling at a single velocity βc , and having an angular phase frequency ω . The charge density is

$$\rho(r, \theta, z) = \lambda_n \delta(z) \delta(r - R) e^{i(n\theta - \omega t)} , \quad (2.1)$$

where λ_n is the line charge density and a cylindrical coordinate has been used (see Fig. 1). The current density has only a θ -component,

$$J_\theta(r, \theta, z) = \lambda_n \beta c \delta(z) \delta(r - R) e^{i(n\theta - \omega t)}. \quad (2.2)$$

Continuity requires $\omega = n\omega_0 = n\beta c/R$, where $\omega_0/2\pi$ is the revolution frequency of the beam particles.

Because a cylindrical coordinate has been chosen, it is most convenient to solve first for electric and magnetic fields along the z -direction, E_z and H_z , which satisfy

$$\left(\nabla^2 + \frac{\omega^2}{c^2} \right) \begin{pmatrix} E_z \\ H_z \end{pmatrix} = 0 \quad (2.3)$$

everywhere inside the beam pipe except at the beam itself. The transverse (to z) fields \vec{E}_t and \vec{H}_t can then be obtained from

$$\begin{aligned} \vec{E}_t \left(1 - \frac{\xi^2 c^2}{\omega^2} \right) &= \frac{c^2}{\omega^2} \vec{\nabla}_t \frac{\partial E_z}{\partial z} + \frac{ic}{\omega} \vec{\nabla}_t \times \hat{z} H_z, \\ \vec{H}_t \left(1 - \frac{\xi^2 c^2}{\omega^2} \right) &= \frac{c^2}{\omega^2} \vec{\nabla}_t \frac{\partial H_z}{\partial z} - \frac{ic}{\omega} \vec{\nabla}_t \times \hat{z} E_z. \end{aligned} \quad (2.4)$$

In above, we have assumed the time-dependence $e^{-i\omega t}$ and the z -dependence $\sin \xi z$ or $\cos \xi z$.

II.2 TM part with perfectly conducting walls

We want to solve for the electromagnetic fields excited by the beam specified by Eqs. (2.1) and (2.2). Then all the fields must have $\exp[i(n\theta - \omega t)]$ behavior with $\omega = n\omega_0 = n\beta c/R$. The fields are divided into the TM part derivable from E_z and the TE part derivable from H_z . Although this division is clear mathematically, care must be exercised to include both contributions in satisfying boundary conditions or matching fields across a charge or current distribution.

From Eq. (2.3), we obtain

$$E_z^{\text{TM}}(r, \theta, z, t) = \sum_{i=1}^{\infty} \pm a_i^{\text{TM}} Z_n(q_i r) \cos \xi_i \left(\frac{h}{2} \mp z \right) \quad z \gtrless 0, \quad (2.5)$$

$$H_z^{\text{TE}}(r, \theta, z, t) = \sum_{i=1}^{\infty} a_i^{\text{TE}} \tilde{Z}_n(q_i r) \sin \xi_i \left(\frac{h}{2} \mp z \right) \quad z \gtrless 0, \quad (2.6)$$

where the $\exp[-in(\theta - \omega_0 t)]$ has been suppressed. The z dependence $\sin \xi_i \left(\frac{h}{2} \mp z \right)$ has been chosen for H_z^{TE} because the vertical magnetic field should vanish at $z = \pm h/2$.

As a result, $E_\theta^{\text{TE}} \sim \partial H_z^{\text{TE}}/\partial r$ will also vanish at $z = \pm h/2$. Then, $E_\theta^{\text{TM}} \sim \partial E_z^{\text{TM}}/\partial z$ must be made to vanish at $z = \pm h/2$ also. The $\cos \xi_i \left(\frac{h}{2} \mp z\right)$ dependence for E_z^{TM} is therefore the correct choice. The signs before the coefficients a_i^{TM} and a_i^{TE} are so chosen that, for the beam at the midplane, E_z^{TM} (H_z^{TE}) should be odd (even) in z .

Let us concentrate on the TM part. The radial wave is

$$Z_n(q_i r) = Y_n(q_i R_-) J_n(q_i r) - J_n(q_i R_-) Y_n(q_i r) , \quad (2.7)$$

where J_n and Y_n are respectively the Bessel function and Neumann function of order n . Note that Z_n , which is proportional to E_z , has been constructed to vanish at the inner radius R_- of the toroidal beam pipe. In order that it will vanish at the outer radius R_+ , we set $q_i R_+$ equal to the i -th zero of $Z_n(x)$. From the wave equation (2.3), ξ_i can then be determined by

$$\xi_i^2 = \left(\frac{n\beta}{R}\right)^2 - q_i^2 .$$

We would like the reader to pay special attention to the terminology used here. The TM and TE imply transverse to the vertical or z -direction but *not* the usual beam direction.

Next, we need to determine the coefficient a_i^{TM} . Before doing so, we must derive the orthonormal relation for $Z_n(q_i r)$. Since $Z_n(q_i r)$ satisfies

$$\frac{1}{r} \frac{\partial}{\partial r} \left[r \frac{\partial}{\partial r} Z_n(q_i r) \right] + \left(q_i^2 - \frac{n^2}{r^2} \right) Z_n(q_i r) = 0 , \quad (2.8)$$

we have for $i \neq j$,

$$\begin{aligned} & (q_i^2 - q_j^2) \int_{R_-}^{R_+} r dr Z_n(q_i) Z_n(q_j) \\ &= \int_{R_-}^{R_+} dr \left\{ Z_n(q_i r) \frac{\partial}{\partial r} \left[r \frac{\partial}{\partial r} Z_n(q_j r) \right] - Z_n(q_j r) \frac{\partial}{\partial r} \left[r \frac{\partial}{\partial r} Z_n(q_i r) \right] \right\} \\ &= r Z_n(q_i r) \frac{\partial}{\partial r} Z_n(q_j r) - r Z_n(q_j r) \frac{\partial}{\partial r} Z_n(q_i r) \Big|_{R_-}^{R_+} , \end{aligned} \quad (2.9)$$

which vanishes for either the Dirichlet or Neumann boundary condition, indicating the orthogonality of $Z_n(q_i r)$. For the normalization, let us take the derivative of Eq. (2.9) with respect to q_i and then let $q_j \rightarrow q_i$ before putting in the limits R_\pm . We get, after making use of Eq. (2.8),

$$2q_i \int_{R_-}^{R_+} r dr Z_n^2(q_i r) = q_i r^2 Z_n'^2(q_i r) + q_i \left(r^2 - \frac{n^2}{q_i^2} \right) Z_n^2(q_i r) \Big|_{R_-}^{R_+} . \quad (2.10)$$

The resulting orthonormal condition can be written as

$$\int_{R_-}^{R_+} r dr Z_n(q_i r) Z_n(q_j r) = \delta_{ij} \bar{R} b \mathcal{N}_i^{\text{TM,TE}} , \quad (2.11)$$

where for the Dirichlet problem or TM modes, the dimensionless normalization constant is

$$\mathcal{N}_i^{\text{TM}} = \frac{1}{2\eta} \left[\frac{R_+^2}{\bar{R}^2} Z_n'^2(q_i R_+) - \frac{R_-^2}{\bar{R}^2} Z_n'^2(q_i R_-) \right] , \quad (2.12)$$

and for the Neumann problem or TE modes,

$$\mathcal{N}_i^{\text{TE}} = \frac{1}{2\eta} \left[\left(\frac{R_+^2}{\bar{R}^2} - \frac{n^2}{q_i^2 \bar{R}^2} \right) \tilde{Z}_n^2(q_i R_+) - \left(\frac{R_-^2}{\bar{R}^2} - \frac{n^2}{q_i^2 \bar{R}^2} \right) \tilde{Z}_n^2(q_i R_-) \right] . \quad (2.13)$$

In above, $\bar{R} = \frac{1}{2}(R_+ + R_-)$ is the average radius of the toroidal beam pipe, $b = \frac{1}{2}(R_+ - R_-)$ is the half width of the beam pipe, and $\eta = b/\bar{R}$. Note that in Eq. (2.13) we have used \tilde{Z}_n defined by Eq. (2.23) below as the radial wave because it satisfies the Neumann boundary condition. If we define a dimensionless radial variable x by

$$r = \bar{R}(1 + \eta x) , \quad (2.14)$$

Eq. (2.11) that defines the dimensionless normalization constants $\mathcal{N}_i^{\text{TM,TE}}$ can be rewritten as

$$\int_{-1}^{+1} dx (1 + \eta x) Z_n^2(x) = \mathcal{N}_i^{\text{TM}} , \quad \int_{-1}^{+1} dx (1 + \eta x) \tilde{Z}_n^2(x) = \mathcal{N}_i^{\text{TE}} . \quad (2.15)$$

The Bessel functions of order n are complete in the r -space, and with the aid of the orthonormal relation, we can write

$$\sum_{i=1}^{\infty} \frac{1}{\mathcal{N}_i^{\text{TM}}} Z_n(q_i r) Z_n(q_i R) = \frac{\eta \bar{R}^2}{R} \delta(r - R) . \quad (2.16)$$

The discontinuity of E_z across $z = 0$ in Eq. (2.5) is related to the charge density of Eq. (2.1) by Gauss's law, which implies

$$\sum_{i=1}^{\infty} 2a_i^{\text{TM}} Z_n(q_i r) \cos \frac{\xi_i h}{2} = 4\pi \lambda_n \delta(r - R) . \quad (2.17)$$

Obviously, only the TM part contributes. Substituting Eq. (2.16) in Eq. (2.17), we get

$$a_i^{\text{TM}} = \frac{2\pi \lambda_n R Z_n(q_i R)}{\eta \bar{R}^2 \mathcal{N}_i^{\text{TM}} \cos \xi_i h / 2} . \quad (2.18)$$

Finally, we obtain for the TM part,

$$E_z(r, \theta, z, t) = \pm 2\pi \lambda_n \frac{R}{\eta R^2} \sum_{i=1}^{\infty} \frac{Z_n(q_i r) Z_n(q_i R)}{\mathcal{N}_i^{\text{TM}}} \frac{\cos \xi_i \left(\frac{h}{2} \mp z \right)}{\cos \xi_i h/2} \quad z \geq 0, \quad (2.19)$$

where again the factor $\exp[-in(\theta - \omega_0)]$ has been suppressed. The transverse TM fields can be obtained easily with the help of Eq. (2.4). Note that Eq. (2.19) will blow up when $\cos \xi_i h/2 = 0$. We will discuss this in Section III.

II.3 TE part with perfectly conducting walls

Let us rewrite H_z for the TE part,

$$H_z^{\text{TE}}(r, \theta, z, t) = \sum_{i=1}^{\infty} a_i^{\text{TE}} \tilde{Z}_n(q_i r) \sin \xi_i \left(\frac{h}{2} \mp z \right) \quad z \geq 0. \quad (2.20)$$

Here, ξ_i is again given by

$$\xi_i^2 = \frac{n^2 \beta^2}{R^2} - q_i^2, \quad (2.21)$$

through Eq. (2.3). However, q_i is not the same as that for the TM part; it is determined from the boundary conditions of the radial magnetic field gotten from Eq. (2.4),

$$H_r(r, \theta, z, t) = H_r^{\text{TM}}(r, \theta, z, t) + H_r^{\text{TE}}(r, \theta, z, t), \quad (2.22)$$

where

$$H_r^{\text{TM}}(r, \theta, z, t) = \pm 2\pi \lambda_n \frac{n\omega R}{c\eta R^2} \sum_{i=1}^{\infty} \frac{Z_n(q_i r) Z_n(q_i R)}{q_i^2 r \mathcal{N}_i^{\text{TM}}} \frac{\cos \xi_i \left(\frac{h}{2} \mp z \right)}{\cos \xi_i h/2} \quad z \geq 0, \quad (2.23)$$

$$H_r^{\text{TE}}(r, \theta, z, t) = \sum_{i=1}^{\infty} \mp \frac{a_i^{\text{TE}} \xi_i}{q_i} \tilde{Z}'_n(q_i r) \cos \xi_i \left(\frac{h}{2} \mp z \right) \quad z \geq 0. \quad (2.24)$$

The radial magnetic field must vanish at $r = R_{\pm}$. This is true for H_r^{TM} . Therefore, we must choose

$$\tilde{Z}_n(q_i r) = Y'_n(q_i R_-) J_n(q_i r) - J'_n(q_i R_-) Y_n(q_i r), \quad (2.25)$$

with $q_i R_+$ equal to the i -th zero of $\tilde{Z}'_n(x)$. Again this q_i is different from that in Eqs. (2.23); the latter is determined by the zeroes of Z_n in Eq. (2.7).

The strength of excitation a_i^{TE} can be obtained from Ampere's law. Equating the discontinuity of H_r in Eq. (2.22) and the beam current in Eq. (2.2), we get

$$\begin{aligned} H_r^{\text{TM}}(r) - \sum_{i=1}^{\infty} \frac{2a_i^{\text{TE}} \xi_i}{q_i} \tilde{Z}'_n(q_i r) \cos \frac{\xi_i h}{2} &= \frac{4\pi}{c} \int J_{\theta} dz \\ &= 4\pi \lambda_n \beta \delta(r - R). \end{aligned} \quad (2.26)$$

We have shown that $\tilde{Z}_n(q_i r)$, being a linear combination of Bessel functions satisfying the Neumann boundary condition, obeys an orthogonality relation,

$$\int_{R_-}^{R_+} \tilde{Z}_n(q_i r) \tilde{Z}_n(q_j r) r dr = 0 \quad i \neq j . \quad (2.27)$$

Differentiating with respect to q_i and q_j , we get

$$\int_{R_-}^{R_+} \tilde{Z}'_n(q_i r) \tilde{Z}'_n(q_j r) r^3 dr = 0 \quad i \neq j . \quad (2.28)$$

We can therefore write

$$\int_{R_-}^{R_+} \tilde{Z}'_n(q_i r) \tilde{Z}'_n(q_j r) r^3 dr = \delta_{ij} \bar{R}^4 \tilde{\mathcal{N}}_i , \quad (2.29)$$

where $\tilde{\mathcal{N}}_i$ is some dimensionless function of $q_i \bar{R}$ and $q_i b$. The strength a_i^{TE} in Eq. (2.26) can now be solved easily; Eq. (2.20) can now be written as

$$\begin{aligned} H_z(r, \theta, z, t) = & - \sum_{i=1}^{\infty} \frac{2\pi \lambda_n \beta q_i R^3}{\xi_i \bar{R}^4} \frac{\tilde{Z}_n(q_i r) \tilde{Z}'_n(q_i R)}{\tilde{\mathcal{N}}_i} \frac{\sin \xi_i \left(\frac{h}{2} \mp z \right)}{\cos \xi_i h/2} \\ & + \sum_{i=1}^{\infty} \frac{q_i F_i^{\text{TM}} \tilde{Z}_n(q_i r)}{2 \xi_i \bar{R}^4 \tilde{\mathcal{N}}_i} \frac{\sin \xi_i \left(\frac{h}{2} \mp z \right)}{\cos \xi_i h/2} \quad z \gtrless 0 , \quad (2.30) \end{aligned}$$

where

$$F_i^{\text{TM}} = \int_{R_-}^{R_+} H_r^{\text{TM}}(r) \tilde{Z}'_n(q_i r) r^3 dr$$

is the contribution of the TM part. Again there is a blowup if $\cos \xi_i h/2 = 0$.

All the transverse fields can now be obtained from Eqs. (2.19) and (2.30). For example, if the longitudinal coupling impedance is desired, E_θ can be computed using Eq. (2.4). It appears that Eqs. (2.19) and (2.30) are very complicated because the q_i in the TM part is different from that in the TE part. However, they are approximately equal at low frequencies and the situation can be simplified tremendously. In fact, we do get back the familiar longitudinal space charge impedance provided that the beam is given a finite size. Fortunately, we will be dealing with toroidal resonances only in this paper and Eqs. (2.19) and (2.30) will not be pursued further.

There is, however, another way to solve for the fields generated by the beam. The toroidal cavity can be divided into two toroids with $r < R$ and $r > R$ instead. The summation will then be over the eigenvalues of the vertical wave function which is the same for the TM and TE parts. The analysis of the coupling impedance at low frequencies will then be very much easier. This analysis will be presented elsewhere.

III. RESONANCES

III.1 The resonant waves

We know that ξ_i is obtained from

$$\xi_i^2 = \frac{n^2 \beta^2}{R^2} - q_i^2, \quad (3.1)$$

where $q_i R_+$ is the i -th zero of $Z_n(x)$ for the TM part or the i -th zero for the TE part. Whenever

$$\xi_i = \frac{\pi(2k-1)}{h} \quad k = 1, 2, \dots, \quad (3.2)$$

$\cos \xi_i h/2 = 0$ and one wave in the summation (2.19) or (2.30) goes to infinity. This is a resonant mode. The infinity comes in because we have treated the beam-pipe wall as perfectly conducting.

Let us examine this particular mode. Substituting Eq. (3.2) in Eq. (2.5) the TM E_z becomes

$$E_z(r, \theta, z, t) = -a_i^{\text{TM}} Z_n(q_i r) \sin \frac{\pi(2k-1)z}{h} \quad (3.3)$$

for all z . Now E_z is analytic across $z = 0$. In fact, this represents a wave in the *empty* beam pipe moving with the same angular velocity and has the same azimuthal variation as the beam. In other words, it is the solution of the *homogeneous* Maxwell's equations but with the same θ and t dependence as the beam. This implies that this wave can propagate by itself in the toroidal beam pipe *without* the presence of the beam. With the presence of the beam, this wave will interact with the beam because it has the same θ and t dependence. Therefore a resonance will be established.

Similar remarks can be made for the TE part. With ξ_i given by Eq. (3.2), the magnetic field in Eqs. (2.20) and (2.24) is analytic across $z = 0$, and the electromagnetic fields form a solution for the *homogeneous* Maxwell's equations. Since these resonances do not require the support of the beam, the TM and TE parts can exist independently. Thus from now on we can talk about TM and TE modes.

Given an i and a k , this resonant wave exists only for the harmonic n that satisfies

$$Z_n(q_i R_+) = 0 \quad \text{and} \quad q_i^2 = \frac{n^2 \beta^2}{R^2} - \frac{\pi^2(2k-1)^2}{h^2} \quad (3.4)$$

for the TM modes, and

$$\tilde{Z}'_n(q_i R_+) = 0 \quad \text{and} \quad q_i^2 = \frac{n^2 \beta^2}{R^2} - \frac{\pi^2(2k-1)^2}{h^2} \quad (3.5)$$

for the TE mode. Therefore, for these resonant modes, we should write ξ_k instead of ξ_i , and the resonant azimuthal harmonic, the solution of Eq. (3.4) or (3.5), should be denoted by n_{ik} .

III.2 Solutions for resonant harmonics

In this section, we try to solve Eq. (3.4) for the TM modes and Eq. (3.5) for the TE modes. The problem is complicated because the harmonic n which we are solving for is the order of the Bessel functions in Z_n or \tilde{Z}_n and it also resides in the argument of Z_n or \tilde{Z}_n through q_i . Observing that n should be much bigger than the cutoff harmonic $n_{co} \sim R/b$ or R/h , we can expand $q_i R_{\pm}$ as

$$\begin{aligned}
q_i R_{\pm} &= \sqrt{\frac{n^2 \beta^2}{R^2} - \frac{\pi^2 (2k-1)^2}{h^2}} R \left(1 \pm \frac{b_{\pm}}{R}\right) \\
&\cong n \left[1 \pm \frac{b_{\pm}}{R} - \frac{1}{2\gamma^2} - \frac{R^2 \pi^2 (2k-1)^2}{2n^2 h^2}\right] \\
&= n[1 \pm \eta_{\pm} - \alpha] \\
&\equiv n z_{\pm},
\end{aligned} \tag{3.6}$$

where

$$b_+ = R_+ - R \quad \text{and} \quad b_- = R - R_- \tag{3.7}$$

are the distances of the beam from, respectively, the inner and outer edge of the beam pipe. The other two quantities, defined as

$$\eta_{\pm} = \frac{b_{\pm}}{R}, \quad \alpha = \frac{1}{2\gamma^2} + \frac{R^2 \pi^2 (2k-1)^2}{2n^2 h^2} \tag{3.8}$$

are much smaller than unity. So $q_i R_{\pm}$ is always very near to n , or $z_{\pm} = q_i R_{\pm}/n$ is very close to unity. Thus, the Bessel functions can be expressed in terms of Airy functions or their derivatives:

$$\begin{aligned}
J_n(nz) &= \left(\frac{4\zeta}{1-z^2}\right)^{1/4} \frac{\text{Ai}(n^{2/3}\zeta)}{n^{1/3}} + O\left(\frac{1}{n^{5/3}}\right), \\
Y_n(nz) &= -\left(\frac{4\zeta}{1-z^2}\right)^{1/4} \frac{\text{Bi}(n^{2/3}\zeta)}{n^{1/3}} + O\left(\frac{1}{n^{5/3}}\right), \\
J'_n(nz) &= -\frac{2}{z} \left(\frac{1-z^2}{4\zeta}\right)^{1/4} \frac{\text{Ai}'(n^{2/3}\zeta)}{n^{2/3}} + O\left(\frac{1}{n^{4/3}}\right), \\
Y'_n(nz) &= \frac{2}{z} \left(\frac{1-z^2}{4\zeta}\right)^{1/4} \frac{\text{Bi}'(n^{2/3}\zeta)}{n^{2/3}} + O\left(\frac{1}{n^{4/3}}\right),
\end{aligned} \tag{3.9}$$

where

$$\begin{cases} \frac{2}{3}\zeta^{3/2} = \ln \frac{1 + \sqrt{1-z^2}}{z} - \sqrt{1-z^2} & z < 1 \\ \frac{2}{3}(-\zeta)^{3/2} = \sqrt{z^2-1} - \cos^{-1} \frac{1}{z} & z > 1. \end{cases} \tag{3.10}$$

Since $z \cong 1$, we find

$$\zeta = 2^{1/3}(1 - z) + O(|1 - z|^{3/2}) . \quad (3.11)$$

Therefore, comparing with Eq. (3.6), we have

$$\zeta_{\pm} = 2^{1/3}(\alpha \mp \eta_{\pm}) , \quad (3.12)$$

where the subscript \pm corresponds to $q_i R_{\pm}$.

Now in terms of Airy functions, Eqs. (3.4) and (3.5) transform into,

$$\text{TM :} \quad \text{Ai}(-y)\text{Bi}(x) - \text{Ai}(x)\text{Bi}(-y) = 0 , \quad (3.13)$$

$$\text{TE :} \quad \text{Ai}'(-y)\text{Bi}'(x) - \text{Ai}'(x)\text{Bi}'(-y) = 0 , \quad (3.14)$$

with

$$\begin{cases} x = 2^{1/3}n^{2/3}(\eta_- + \alpha) \\ y = 2^{1/3}n^{2/3}(\eta_+ - \alpha) . \end{cases} \quad (3.15)$$

Equations (3.13) and (3.14) can be rewritten as,

$$\text{TM :} \quad \frac{\text{Ai}(x)}{\text{Bi}(x)} = \frac{\text{Ai}(-y)}{\text{Bi}(-y)} , \quad (3.16)$$

$$\text{TE :} \quad \frac{\text{Ai}'(x)}{\text{Bi}'(x)} = \frac{\text{Ai}'(-y)}{\text{Bi}'(-y)} . \quad (3.17)$$

We see from Fig. 2 that, when $x > 0$, $\text{Ai}(x)/\text{Bi}(x)$ and $\text{Ai}'(x)/\text{Bi}'(x)$ are monotonic and decay to zero exponentially. Thus Eq. (3.16) or Eq. (3.17) will have no solution if both x and $-y$ are positive aside from the trivial one $x = y = 0$. Since x is positive [Eq. (3.15)], to arrive at a solution, we must have y positive or $\eta_+ > \alpha$. Note that this condition is equivalent to criterion (1.1), because at the limit of the criterion n_{11}^{TM} or n_{11}^{TE} goes to infinity (see below) and the second term of α in Eq. (3.8) vanishes. Under this situation, the left sides of Eqs. (3.16) are exponentially decaying, but the right sides are monotonically increasing and resemble the tangent curves having zeros and reaching $\pm\infty$. Since

$$\frac{x}{y} = \frac{\eta_- + \alpha}{\eta_+ - \alpha} > 1 , \quad (3.18)$$

when the right sides of Eq. (3.16) and Eq. (3.17) reach their respective zeroes, the left sides have already decayed to zero practically. Thus, to a high degree of accuracy, the solutions are (see Fig. 2):

$$\text{TM :} \quad \text{Ai}(-y) = 0 , \quad (3.19)$$

$$\text{TE :} \quad \text{Ai}'(-y) = 0 . \quad (3.20)$$

Therefore the resonant harmonics are given by

$$2^{1/3}n_{ik}^{2/3} \left[\frac{b_+}{R} - \frac{1}{2\gamma^2} - \frac{R^2\pi^2(2k-1)^2}{2n_{ik}^2h^2} \right] = \begin{cases} y_i & \text{TM} \\ y'_i & \text{TE} \end{cases}, \quad (3.21)$$

where $-y_i$ and $-y'_i$ are respectively the i th zeroes of $\text{Ai}(-y)$ and $\text{Ai}'(-y)$, the first few of which are listed in Table I. Since $\text{Ai}(-y)$ starts off positive at $y = 0$ and $\text{Ai}'(-y)$

TM modes	TE modes
$y_1 = 2.3381$	$y'_1 = 1.0188$
$y_2 = 4.0879$	$y'_2 = 3.2482$
$y_3 = 5.5205$	$y'_3 = 4.8201$
$y_4 = 6.7867$	$y'_4 = 6.1633$
$y_5 = 7.9441$	$y'_5 = 7.3722$
$y_6 = 9.0227$	$y'_6 = 8.4885$

Table I: Zeroes of $\text{Ai}(-y)$ and $\text{Ai}'(-y)$.

starts off negative at $y = 0$, it is obvious that the lowest resonant wave is a TE mode.

The accuracy of the solutions can be improved straightforwardly by iterations of Eqs. (3.13) and (3.14) and by including more terms in Eq. (3.9). However, higher accuracy is not meaningful because firstly the cross section of the beam pipe is not exactly rectangular and secondly the toroidal ring is not perfectly round.

In most cases, $n_{ik} \gg (R^3/bh^2)^{1/2} \sim n_{co}^{3/2}$, the last term on the left side of Eq. (3.21) can be neglected, and the solution can then be simplified to

$$\frac{R_+\beta}{R} = \begin{cases} 1 + y_i 2^{-1/3} n_{ik}^{-2/3} & \text{TM} \\ 1 + y'_i 2^{-1/3} n_{ik}^{-2/3} & \text{TE} \end{cases}. \quad (3.22)$$

The lowest mode is

$$\frac{R_+\beta}{R} = 1 + 0.8086 n_{1k}^{-2/3}, \quad (3.23)$$

which is the first TE mode. This is the formula given by Faltens and Laslett.² With the beam roughly at the center of the beam pipe, $R \sim \bar{R}$, this lowest resonant harmonic reduces to

$$n_{1k}^{\text{TE}} = 1.375 \left(\frac{\bar{R}}{b} \right)^{3/2} = O(n_{co}^{3/2}). \quad (3.24)$$

Note that formula (3.22) may not be accurate for the lowest modes.

For the SSC, if we take $b = h/2 = 1.5$ cm, $\bar{R} = 13200.95$ m, the lowest TM and TE resonant harmonics at 20 TeV ($\gamma = 20,000$ has been used) are respectively

$$\begin{aligned} n_{11}^{\text{TM}} &= 2.57 \times 10^9 \\ n_{11}^{\text{TE}} &= 1.40 \times 10^9, \end{aligned} \quad (3.25)$$

which differ by quite a bit from the results of the approximate formulas (3.22), $n_{1k}^{\text{TM}} = 2.09 \times 10^9$ and $n_{1k}^{\text{TE}} = 6.01 \times 10^8$, although the orders of magnitude are correct.

The field distributions in the radial direction are plotted in Figs. 3 and 4 respectively for the lowest TM and TE modes. We see that the fields are always concentrated in a region between the beam and the outer edge of the beam pipe, where the linear velocity can be larger than c . Therefore, the wavelength should be much less than the size of the pipe. As γ decreases, the resonant fields are pushed more and more towards the outer edge of the pipe in order to attain the velocity of light. As a result the wavelength decreases or the resonant azimuthal harmonic n_{11}^{TM} or n_{11}^{TE} increases. When the beam velocity drops to the limit of criterion (1.1), the available region for propagation inside the pipe is squeezed to zero and n_{11}^{TM} or n_{11}^{TE} will be pushed to infinity. For this reason, Faltens-Laslett's formula (3.22) will be accurate only at low beam momenta when n_{11}^{TM} or n_{11}^{TE} is large enough so that the third term in Eq. (3.21) can be neglected.

Harmonics of other modes are tabulated in Table II. For comparison, the cutoff harmonics for this rectangular beam pipe are $n_{\text{co}}^{\text{TM}} = 1.95 \times 10^6$ and $n_{\text{co}}^{\text{TE}} = 1.38 \times 10^6$, and the the revolution frequency is 3.61 kHz. However, for these cutoff harmonics the TM and TE imply transverse to the beam direction, which are different from the TM and TE defined in this paper. The cutoff harmonic for a circular beam pipe of radius 1.5 cm is $n_{\text{co}} = 2.12 \times 10^6$.

It is interesting to note that our approximate solutions of the resonant frequencies in Eq. (3.21) do not depend on the radius of the inner edge of the beam pipe R_- . The only requirement is that the radial distance of the beam from the outer edge of the beam pipe is small compared with the radius of the outer edge; or $b_+ \ll R_+$. In fact, we can reduce R_- to zero and have the same solutions. Under this situation, the toroidal beam pipe cavity reduces to a cylindrical cavity of radius R_+ and height h . The reason is very clear upon examining the fields in Figs. 3 and 4. At resonance, these fields are pushed towards a small region near the outer edge of the beam pipe and are vanishingly small near the inner edge. As a result, it does not matter at all whether the inner boundary of the beam pipe is present or not.

It is worthwhile to point out that the harmonic n must be an integer. However, it has been treated as a continuous variable in the solution of the resonance modes.

Theoretically, the possibility that a solution lands at an exact integer is zero. Therefore, in the ideal situation of a toroidal cavity with infinitely conducting walls, there is no legitimate solution at all. In other words, the resonances with non-integer n which we have solved above are mathematical in nature only. They do not exist and will no affect the beam at all. However, when wall resistivity is introduced, each resonance will have a finite spread and will certainly cover some integers. Thus excitation becomes possible.

IV. MODEL WITH FINITE WALL CONDUCTIVITY

IV.1 Figure of merit

If we introduce a finite wall conductivity σ , each resonance will no longer be infinite and has a finite width. The sharpness of the resonance is described by the figure of merit Q_{ik}^{TM} or Q_{ik}^{TE} , which can be estimated from the volume and surface area of the beam-pipe cavity

$$Q \sim \frac{2}{\delta} \frac{\text{volume}}{\text{surface area}}, \quad (4.1)$$

where δ is the skin depth into the pipe wall. For our rectangular toroidal beam pipe, this estimate becomes (in mks units)

$$Q \sim \sqrt{\frac{Z_0 n \sigma}{2R}} \frac{2bh}{2b+h}, \quad (4.2)$$

where $Z_0 = 377 \Omega$ is the impedance of free space. Taking copper at 4°K or $\sigma = 1.80 \times 10^9 (\Omega\text{-m})^{-1}$, we get $Q \sim 76.0\sqrt{n}$. Therefore the lowest resonance at ~ 20 TeV has $Q_{11}^{\text{TE}} \sim 2.84 \times 10^6$ or a FWHM spread of $\Delta n_{11}^{\text{TE}} = n_{11}^{\text{TE}}/Q_{11}^{\text{TE}} \sim 492$.

A more accurate definition of Q is 2π times the ratio of the time-averaged energy stored to the energy loss per cycle. The power lost to the wall is

$$\begin{aligned} \bar{P} &= \left[\frac{c}{4\pi} \right] \frac{1}{2} \oint_S \vec{E}_a \times \vec{H}_a^* \cdot \hat{n} dS \\ &= \left[\frac{c}{4\pi} \right] \frac{\delta_a \omega_a \mu_c}{4c} \oint_S (\vec{H}_a \times \hat{n}) \cdot (\vec{H}_a^* \times \hat{n}) dS \\ &= \frac{\delta_a \omega_a \mu_c}{16\pi} \oint_S |\vec{H}_a|^2 dS, \end{aligned} \quad (4.3)$$

where the subscript a stands for the resonance ik of either the TM or TE mode, $\mu_c \sim 1$ is the relative magnetic permeability of the pipe wall, and the integrals are carried over the walls of the beam pipe. In writing down Eq. (4.3), we have made the approximation that the resonances are widely separated.

We next normalized the electric and magnetic fields of mode a by letting

$$\vec{E}_a = e_a \vec{\mathcal{E}}_a, \quad \vec{H}_a = h_a \vec{\mathcal{H}}_a, \quad (4.4)$$

so that the volume integrals

$$\oint_V |\vec{\mathcal{E}}_a|^2 dV = \oint_V |\vec{\mathcal{H}}_a|^2 dV = 1. \quad (4.5)$$

Here e_a and h_a represent the strengths of the excitation and they are related. For example, if we take the absolute value squared of Faraday's law,

$$e_a \vec{\nabla} \times \vec{\mathcal{E}}_a = \frac{i\omega}{c} h_a \vec{\mathcal{H}}_a, \quad (4.6)$$

and integrate over the whole volume of the cavity, with the help of Eqs. (2.3) and (4.5), it is easy to find $|e_a| = |h_a|$ in the Gaussian units. Note that we can still have an arbitrary choice of relative phase.

The energy stored in the toroidal ring in this mode is

$$\varepsilon_a = \frac{1}{8\pi} |e_a|^2 = \frac{1}{8\pi} |h_a|^2. \quad (4.7)$$

The figure of merit is therefore by definition,

$$Q_a = \frac{2}{\mu_c \delta_a} \frac{1}{\oint_S |\vec{\mathcal{H}}_a|^2 dS}. \quad (4.8)$$

For the (ik) -th TM mode, using Eqs. (3.3) and (2.4), the normalized fields are

$$\begin{aligned} (\mathcal{E}_{ik})_z &= \frac{q_i R}{\sqrt{\pi h \eta \mathcal{N}_{ik}^{\text{TM}} n \bar{R} \beta}} Z_n(q_i r) \sin \xi_k z, \\ (\mathcal{E}_{ik})_r &= \frac{\xi_k R}{\sqrt{\pi h \eta \mathcal{N}_{ik}^{\text{TM}} n \bar{R} \beta}} Z'_n(q_i r) \cos \xi_k z, \\ (\mathcal{E}_{ik})_\theta &= \frac{i \xi_k R}{\sqrt{\pi h \eta \mathcal{N}_{ik}^{\text{TM}} q_i \bar{R} \beta}} \frac{Z_n(q_i r)}{r} \cos \xi_k z, \\ (\mathcal{H}_{ik})_r &= \frac{n}{\sqrt{\pi h \eta \mathcal{N}_{ik}^{\text{TM}} q_i \bar{R}}} \frac{Z_n(q_i r)}{r} \sin \xi_k z, \\ (\mathcal{H}_{ik})_\theta &= \frac{i}{\sqrt{\pi h \eta \mathcal{N}_{ik}^{\text{TM}} \bar{R}}} Z'_n(q_i r) \sin \xi_k z, \end{aligned} \quad (4.9)$$

where $\xi_k = \pi(2k - 1)/h$, $\mathcal{N}_{ik}^{\text{TM}}$ is given by Eq. (2.12), and $n = n_{ik}^{\text{TM}}$ is the resonant harmonic. Again, the θ and t dependences have been suppressed. Then,

$$\oint_S |\vec{\mathcal{H}}_{ik}|^2 dS = \frac{4}{h} + \frac{2}{R} \frac{(R_+/R)Z_n'^2(q_i R_+) + (R_-/R)Z_n'^2(q_i R_-)}{(R_+/R)^2 Z_n'^2(q_i R_+) - (R_-/R)^2 Z_n'^2(q_i R_-)}. \quad (4.10)$$

Note that the second term, the contribution of the inner and outer curved surfaces, is very much less than the first term which comes from the top and bottom flat walls. Thus, retaining only the latter contribution,

$$Q_{ik}^{\text{TM}} \approx \frac{h}{2\delta_{ik}}, \quad (4.11)$$

which is close to our estimate of (4.2).

For the (ik) -th TE mode, the normalized fields are

$$\begin{aligned} (\mathcal{H}_{ik})_z &= \frac{q_i R}{\sqrt{\pi h \eta \mathcal{N}_{ik}^{\text{TE}} n \bar{R} \beta}} \tilde{Z}_n(q_i r) \cos \xi_k z, \\ (\mathcal{H}_{ik})_r &= -\frac{\xi_k R}{\sqrt{\pi h \eta \mathcal{N}_{ik}^{\text{TE}} n \bar{R} \beta}} \tilde{Z}'_n(q_i r) \sin \xi_k z, \\ (\mathcal{H}_{ik})_\theta &= \frac{i \xi_k R}{\sqrt{\pi h \eta \mathcal{N}_{ik}^{\text{TE}} q_i \bar{R} \beta}} \frac{\tilde{Z}_n(q_i r)}{r} \sin \xi_k z, \\ (\mathcal{E}_{ik})_r &= -\frac{n}{\sqrt{\pi h \eta \mathcal{N}_{ik}^{\text{TE}} q_i \bar{R}}} \frac{\tilde{Z}_n(q_i r)}{r} \cos \xi_k z, \\ (\mathcal{E}_{ik})_\theta &= -\frac{i}{\sqrt{\pi h \eta \mathcal{N}_{ik}^{\text{TE}} \bar{R}}} \tilde{Z}'_n(q_i r) \cos \xi_k z, \end{aligned} \quad (4.12)$$

where $\xi_k = \pi(2k - 1)/h$, $\mathcal{N}_{ik}^{\text{TE}}$ is given by Eq. (2.13), and $n = n_{ik}^{\text{TE}}$ is the resonant harmonic. Then,

$$\begin{aligned} \oint_S |\vec{\mathcal{H}}_{ik}|^2 dS = & \frac{4\xi_k^2}{n^2 \beta^2 \eta q_i^2 h} \left\{ \frac{Rh}{4\bar{R}\mathcal{N}_{ik}^{\text{TE}}} \left[\left(\frac{n^2}{R_+} + \frac{q_i^4 R_+}{\xi_k^2} \right) \tilde{Z}_n^2(q_i R_+) + \left(\frac{n^2}{R_-} + \frac{q_i^4 R_-}{\xi_k^2} \right) \tilde{Z}_n^2(q_i R_-) \right] \right. \\ & \left. + \eta q_i^2 R^2 \right\}, \end{aligned} \quad (4.13)$$

where the first two terms are the outer and inner curved wall contributions while the third term comes from the upper and lower walls. Note that $q_i R \approx q_i R_\pm \approx n$ and

$\xi_k R \sim n_{\text{co}}$. For the two terms n^2/R_{\pm} and $q_i^4 R_{\pm}/\xi_k^2$, the ratio is

$$\frac{n^2 \xi_k^2}{R_{\pm}^2 q_i^4} \sim \left(\frac{n_{\text{co}}}{n}\right)^2 \ll 1, \quad (4.14)$$

so that the n^2/R_{\pm} terms can be neglected. The last term is

$$\frac{4\xi_k^2 R^2}{n^2 \beta^2 h} \sim \frac{4}{h} \left(\frac{n_{\text{co}}}{n}\right)^2 \ll \frac{4}{h}. \quad (4.15)$$

Thus the main contribution comes from the $q_i^4 R_{\pm}/\xi_k^2$ terms, or the curved surfaces only. At resonance, the normalization constants $\mathcal{N}_{ik}^{\text{TE}}$ and $\mathcal{N}_{ik}^{\text{TM}}$ given by Eqs. (2.12) and (2.13) can be simplified using the resonance condition of Eq. (3.4) or (3.5) as well as the Wronskian for $J_n(x)$ and $Y_n(x)$. The results are

$$\mathcal{N}_{ik}^{\text{TE}} = \frac{2}{\pi^2 Q_i^2 R b} \left[\left(1 - \frac{n^2}{q_i^2 R_+^2}\right) \left(\frac{Y_n'(q_i R_-)}{Y_n'(q_i R_+)}\right)^2 - \left(1 - \frac{n^2}{q_i^2 R_-^2}\right) \right], \quad (4.16)$$

and

$$\mathcal{N}_{ik}^{\text{TM}} = \frac{2}{\pi^2 Q_i^2 R b} \left[\left(\frac{Y_n(q_i R_-)}{Y_n(q_i R_+)}\right)^2 - 1 \right]. \quad (4.17)$$

Similarly, $\tilde{Z}_n(q_i R_{\pm})$ in Eq. (4.13) can be simplified. Remember that the fields in a resonance are pushed mostly to the outer pipe boundary or the contribution of the inner wall is negligible compared with that of the outer wall. Mathematically, this is equivalent to

$$\frac{\tilde{Z}_n^2(q_i R_+)}{\tilde{Z}_n^2(q_i R_-)} \gg 1 \quad \text{and} \quad \frac{Y_n'^2(q_i R_-)}{Y_n'^2(q_i R_+)} \gg 1.$$

Then, Eq. (4.13) reduces to

$$\oint_S |\vec{\mathcal{H}}_{ik}|^2 dS \approx \frac{1}{b} \left(1 - \frac{\alpha}{\eta}\right)^{-1}, \quad (4.18)$$

and therefore

$$Q_{ik}^{\text{TE}} \approx \frac{2b}{\delta_{ik}} \left(1 - \frac{\alpha}{\eta}\right), \quad (4.19)$$

where η ($\approx \eta_{\pm}$) and α are given by Eq. (3.8). Although α/η is not negligible, it is usually small for higher resonance modes and at high energies. As a result, Q_{ik}^{TE} turns out to give roughly the order of magnitude as Eq. (4.2).

It is interesting to note that Q_{ik}^{TM} receives its contribution mainly from the top and bottom flat walls and is therefore proportional to the height h of vacuum chamber. On the other hand, Q_{ik} relies mostly on the contribution from the outer curved wall, it is therefore proportional approximately to b , the distance from the beam to the outer wall.

IV.2 Shunt impedance

We first compute the amount of fields of the a -th mode, e_a or h_a in Eq. (4.4) excited by the beam by assuming a power loss in the pipe walls. Then the shunt impedance can be inferred.

From Eqs. (4.3) and (4.8), the average power lost to the pipe wall for mode a is

$$\bar{P} = \left[\frac{1}{4\pi} \right] \frac{\omega_a}{2Q_a} |h_a|^2 . \quad (4.20)$$

The power loss can also be computed by the azimuthal electric field $(\mathcal{E}_\theta)_a$ seen by the beam current I

$$\bar{P} = \frac{1}{2} e_a \oint (\mathcal{E}_\theta)_a I^* dl . \quad (4.21)$$

Equating Eqs. (4.20) and (4.21) and recalling that $|e_a| = |h_a|$, we get

$$e_a^* = -\frac{4\pi Q_a}{\omega_a} \oint (\mathcal{E}_\theta)_a I^* dl . \quad (4.22)$$

Denoting the ‘voltage’ dropped per unit current by

$$\phi_a = \frac{\oint (\mathcal{E}_\theta)_a I^* dl}{|I|} \quad (4.23)$$

and substituting e_a^* into Eq. (4.21), the average power loss becomes

$$\bar{P} = \frac{2\pi Q_a}{\omega_a} |I|^2 |\phi_a|^2 . \quad (4.24)$$

Therefore the shunt impedance or the impedance at ω_a is

$$Z_{\text{sh}} = \frac{4\pi Q_a}{\omega_a} |\phi_a|^2 . \quad (4.25)$$

In mks units, this is

$$Z_{\text{sh}} = Z_0 \frac{cQ_a}{\omega_a} |\phi_a|^2 . \quad (4.26)$$

Thus what we need to compute is ϕ_a defined in Eq. (4.23) which is just the integral of $(\mathcal{E}_\theta)_a$ along the beam orbit. Using the explicit expressions given in Eqs. (4.9) and (4.12), we obtain

$$|\phi_a|^2 = \begin{cases} \frac{4\pi R \xi_a^2}{hbq_a^2 \beta^2} \frac{|Z_{n_a}|_{\text{beam}}^2}{\mathcal{N}_a^{\text{TM}}} & \text{TM} , \\ \frac{4\pi R}{hb^3 q_a^2} \frac{|d\tilde{Z}_{n_a}/dx|_{\text{beam}}^2}{\mathcal{N}_a^{\text{TE}}} & \text{TE} , \end{cases} \quad (4.27)$$

where, in $d\tilde{Z}_{n_a}/dx$, \tilde{Z}_{n_a} is considered as a function of x defined by $r = \bar{R} + bx$. Recalling that $q_a R \approx n_a$, we get for the shunt impedance per unit harmonic (in mks units),

$$\frac{Z_{\text{sh}}}{n} \cong \begin{cases} \frac{4\pi^3 Z_0 Q_a (2k-1)^2 R^4 |Z_{n_a}|_{\text{beam}}^2}{n_a^4 h^3 b \mathcal{N}_a^{\text{TM}}} & \text{TM,} \\ \frac{4\pi Z_0 Q_a R^4 |d\tilde{Z}_{n_a}/dx|_{\text{beam}}^2}{n_a^4 h b^3 \mathcal{N}_a^{\text{TE}}} & \text{TE,} \end{cases} \quad (4.28)$$

where $\mathcal{N}_a^{\text{TM}}$ and $\mathcal{N}_a^{\text{TE}}$ are given by Eqs. (4.16) and (4.17). Again the contributions of the TM (TE) modes come mainly from the upper and lower planar walls (outer curved wall).

As an illustration for the SCC, using $b = h/2 = 1.5$ cm and wall conductivity (copper at 4°K) $\sigma = 1.8 \times 10^9$ (Ωm)⁻¹, the Q 's and Z_{sh}/n for the lowest TM and TE modes at ~ 1 TeV and ~ 20 TeV are listed in Table III. Aside from the field form factors which are the last factors in the Z_{sh} formulas of Eq. (4.28), $Z_{\text{sh}}/n \sim n^{-7/2}$ and $Q \sim n^{1/2}$.

	1 TeV		20 TeV	
	TE	TM	TE	TM
n_a	2.33×10^9	5.39×10^9	1.40×10^9	2.57×10^9
f_a	8.42×10^3 GHz	1.95×10^4 GHz	5.05×10^3 GHz	9.28×10^3 GHz
Q_a	2.97×10^6	5.58×10^6	3.25×10^6	3.85×10^6
$\frac{Z_{\text{sh}}}{n}$	7.45×10^{-5} Ω	2.07×10^{-7} Ω	8.36×10^{-4} Ω	1.22×10^{-4} Ω
$\frac{Z_{\text{sh}}}{n} \Big _{\text{eff}}$	5.84×10^{-2} Ω	2.00×10^{-4} Ω	3.59×10^{-1} Ω	8.10×10^{-2} Ω

Table III: Impedances and positions of the lowest TE and TM modes

V. EFFECTIVE IMPEDANCE

We have seen that a particle beam revolving along an orbit of a certain radius R will excite a series of TM and TE resonances centered at harmonics n_{ik}^{TM} and n_{ik}^{TE} . For particles traveling at a slightly different radius $R + \Delta R$, another series of resonances will be excited at slightly different harmonics. We want to compute the ΔR which will excite the resonance at the next harmonic, i.e., $n = n_{ik} + 1$ where the superscript TM or TE has been suppressed.

We need the beam position R as an implicit function of the particle velocity β and resonant harmonic n_{ik} . This can be obtained by rewriting Eq. (3.21) as

$$\frac{R_+\beta}{R} = 1 + a_i n_{ik}^{-2/3} + \frac{R^2 \xi_k^2}{2n_{ik}^2}, \quad (5.1)$$

where a_i are related to the zeroes of the Airy function or its derivative,

$$a_i = \begin{cases} 2^{-1/3} y_i & \text{TM} \\ 2^{-1/3} y_i' & \text{TE} \end{cases}. \quad (5.2)$$

Differentiating Eq. (5.1), one obtains

$$\left(\frac{\eta_p}{\alpha_p} + \frac{R^2 \xi_k^2}{n_{ik}^2} \right) \frac{\Delta R}{R} = \frac{R}{R_+\beta} \left(\frac{2}{3} a_i n_{ik}^{-5/3} + \frac{R^2 \xi_k^2}{n_{ik}^3} \right), \quad (5.3)$$

where η_p is the frequency dispersion and α_p is the momentum compaction. The SSC main ring will be operated well above transition; therefore $\eta_p \cong \alpha_p$. Keeping only the lowest-order terms, Eq. (5.3) can be simplified to

$$\Delta R \cong \frac{2}{3} \left(\frac{b}{n_{ik}} + \frac{R^3 \xi_k^2}{n_{ik}^3} \right), \quad (5.4)$$

where b is the half width of the beam pipe. For the lowest TE mode which occurs at ~ 20 TeV, $n_{11}^{\text{TE}} = 1.40 \times 10^9$. Taking $b = 1.5$ cm, we get

$$\Delta R = 1.32 \times 10^{-11} \text{ m}, \quad (5.5)$$

which the radial offset of the particle beam to excite the lowest resonance at the next harmonic. If we use the simplified Faltens-Laslett's formula of Eq. (3.23) instead, we will obtain only the first term in Eq. (5.4).

The SSC main ring is designed to have a longitudinal momentum spread of $\Delta p/p \sim 10^{-4}$ to avoid transverse instability. It has a frequency dispersion of $\eta_p = 0.000233$. Therefore the transverse half beam size is $R\eta_p \Delta p/p \sim 2.9 \times 10^{-4}$ m. From the designed

normalized transverse emittance $\epsilon_n = 1.0 \times 10^{-6} \pi$ m-rad, we get a transverse half beam size of 4.5×10^{-4} m if an average beta-function of 200 m is assumed. Thus, radially across the beam of radius ~ 0.4 mm, a total of

$$N = \frac{\text{beam size}}{\Delta R} \sim 6.1 \times 10^7 \quad (5.6)$$

series of resonances can be excited. In other words, for a given ik of either the TE or TM mode, the resonances cover a range of harmonics of width $\sim 10^8$.

We have shown in Section IV.1 that the lowest resonance has a FWHM of

$$\Delta n_{11}^{\text{TE}} = \frac{n_{11}^{\text{TE}}}{Q_{11}^{\text{TE}}} \sim 430, \quad (5.7)$$

where the more accurate Q_{11}^{TE} in Table III has been used. This implies that each particle beam of a definite radius in the SSC can excite ~ 430 lowest TE resonances. We therefore make the proposition that the effective impedance per harmonic of the a -th resonance seen by the beam should be Z_{sh}/n multiplied by the resonance width n_a/Q_a ; or

$$\frac{Z_{\text{sh}}}{n} \Big|_{\text{eff}} \sim \left(\frac{Z_{\text{sh}}}{n} \right) \left(\frac{n_a}{Q_a} \right) = \frac{Z_{\text{sh}}}{Q_a}. \quad (5.8)$$

Here we have violated the condition that the resonances are far apart or isolated. Therefore, Eq. (5.8) may not be correct at all. However, it should give us a correct estimate. The results are tabulated in the last row of Table III. We see that for the lowest resonance $|Z/n|_{\text{eff}} \sim 0.36 \Omega$ which is not too small. However, recalling that the SSC bunch has a rms length of 7 cm, the bunch spectrum extends to a rms harmonic of only 1.89×10^5 , whereas the resonance is at $n_{11}^{\text{TE}} = 2.33 \times 10^9$. Therefore this impedance should have negligible effect on bunch-mode stability. The effective impedance of this lowest mode, being a broad band of harmonic width $\sim 6 \times 10^7$ much bigger than the spread of the bunch spectral harmonic, can drive a fast microwave growth.⁴ But there is no alarm because the designed spread in momentum $\Delta p/p \sim 10^{-4}$ warrants the Landau damping⁵ of the growth driven by an impedance per unit harmonic of 15Ω which is much larger than what we have here. The effective impedances of other higher modes are listed in Table III.

A better approach may be to start from summing up the azimuthal electric fields \mathcal{E}_θ due to these adjacent resonances and then compute the effective impedance.⁶ Since the azimuthal electric fields for these resonances may not be in phase, the actual impedance computed will be less than that given by Eq. (5.8).

Next let us consider moving the beam sideway from the center of the beam pipe. Let the fractional displacement outward be Δ . If the beam is at the inner edge of the beam pipe, $\Delta = -1$, the form factor, which is defined as the last factor in Eq. (4.28),

vanishes because the radial wave $Z(qr)$ or $\tilde{Z}'(qr)$ is zero there. As the beam is moved outward keeping the linear velocity constant, the form factor increases and so does the resonant harmonic because the allowable space for the field becomes less and less. Due to criterion (1.1), the allowable space vanishes and there is no resonance possible when Δ reaches

$$\Delta_m = 1 - \frac{\bar{R}}{2\gamma^2 b}. \quad (5.9)$$

At this point the resonant harmonic reaches infinity and the form factor drops to zero. Thus, the effective impedance given by Eq. (4.28) rises from zero at the inner edge of the pipe, attains a maximum, and drops to zero at Δ_m which is 0.56 and 0.9989 when $\gamma = 1000$ and 20000 respectively. The results are plotted in Fig. 5. We see that when γ is not too big, for example ~ 1000 , the impedance can be reduced by pushing the beam outward from the center of the pipe so that the region available for wave propagation is reduced. On the other hand, when γ is extremely large, for example ~ 20000 , the impedance can be reduced by pushing the beam inward so that the form factor or the interaction between the beam and the resonant wave becomes smaller.

VI. APPLICATIONS TO THE SSC BOOSTERS AND THE TEVATRON

VI.1 The SSC injectors

The injection system of the SSC consists of three boosters: the low energy booster (LEB), the medium energy booster (MEB), and the high energy booster (HEB). Some specifications of these booster rings are listed in Table IV.

	LEB	MEB	HEB
Ring radius	39.73 m	302.52 m	954.93
Beam pipe radius	10 cm	10 cm	6.5 cm
γ (injection)	1.632	8.585	106.6
γ (extraction)	8.585	106.6	1065

Table IV: Sizes and injection and extraction γ 's of the SSC injectors

According to criterion (1.1), in order to have toroidal resonances, the minimum γ 's required are 14.1, 38.9, and 85.7 respectively, where we have assumed that the

beam is at the center of the beam pipe. Therefore, we expect no such resonances will occur in the LEB. In Table V, we list the lowest resonances (TE modes) for the MEB and HEB at extraction energies, where the impedances are largest. The conductivity of stainless steel, $\sigma = 1.37 (\Omega\text{-m})^{-1}$ is assumed.

	MEB	HEB
n_a	3.17×10^5	3.03×10^6
f_a	5.00×10^1 GHz	1.51×10^2 GHz
Q_a	5.48×10^4	6.70×10^4
$\frac{Z_{sh}}{n}$	0.769 Ω	0.0609 Ω
$\frac{Z_{sh}}{n} \Big _{\text{eff}}$	4.45 Ω	2.75 Ω

Table V: Impedances and positions of the lowest modes for the MEB and HEB

The MEB has a bunch length of 0.14 m corresponding to an rms harmonic spectral spread of 2.1×10^3 which is about 150 times less than the harmonic of the lowest toroidal resonance. The limit for mode-colliding instability⁷ is quite high, $|\text{Im } Z/n| \sim 73 \Omega$. The fast microwave limit⁷ is $Z/n \sim 13 \Omega$. A rms bunch area of 0.0018π eV-sec, a rms energy spread of 3.8×10^{-5} , and a bunch intensity of 2×10^{10} particles have been assumed. In any case, no worry of instability is necessary.

For the HEB, the limits⁷ for mode-colliding and fast microwave instabilities are $|\text{Im } Z/n| \sim 1.89 \Omega$ and $Z/n \sim 0.33 \Omega$ respectively. A rms bunch area of 0.0018π eV-sec, a rms energy spread of 1.3×10^{-5} , and a bunch intensity of 2×10^{10} particles have been assumed. The HEB has a bunch length of 0.04 m, corresponding to a rms harmonic spectral spread of 2.3×10^4 which is about 130 times less than the harmonic of the lowest toroidal resonance. Thus, mode-colliding stability may be safe but microwave growth is not. At the very end of the cycle, the bunch area is blown up to 0.035π eV-sec. The stability limits will be increased by ~ 86 times and the bunch will become very stable. However, we think that it is necessary to increase the bunch area in the whole acceleration cycle to safeguard stability.

The HEB is superconducting. Let us consider for fun if the beam pipe were coated with a layer of copper in the same way as the main ring. The wall conductivity will

become $\sigma = 1.8 \times 10^9 (\Omega\text{-m})^{-1}$ which is 1310 times bigger. In the last column of Table V, Q_a becomes 2.43×10^6 and Z_{sh}/n becomes 2.21Ω . We see that, unlike the SSC main ring, due to the much larger ratio of beam-pipe radius to ring radius, the resonance observed here (and for higher modes also) is very narrow indeed. The spread in harmonics is only ~ 1.25 . The criterion for fast microwave stability driven by resonances narrower than the spectral width of the bunch is⁸

$$\frac{Z_{\text{sh}}}{Q} \leq \frac{4|\eta_p|E/e}{\beta^2 I_{av}} \left(\frac{\sigma_E}{E} \right)^2, \quad (6.1)$$

where η_p is the frequency dispersion and σ_E/E is the rms energy spread. Note that the *average* bunch current I_{av} has been used instead and Z_{sh}/Q is just the effective Z/n defined in Eq. (5.8). Taking $\eta_p = 0.002772$, $\sigma_E/E = 1.3 \times 10^{-5}$, we obtain the limit $Z_{\text{sh}}/Q = 11000 \Omega$. This indicates that reducing the wall resistivity of the beam pipe can help a lot under some special situation.

VI.2 The TEVATRON

The TEVATRON is very similar to the HEB of the SCC both in size and energy. The ring radius is 1 km, the beam pipe radius 3.1 cm, and the injection and extraction energies are 150 GeV and 1 TeV respectively. The lowest toroidal resonant modes are listed in Table VI. A wall conductivity of $\sigma = 1.37 \times 10^6 (\Omega\text{-m})^{-1}$ is assumed.

The colliding mode of the TEVATRON is designed to store proton and antiproton bunches of intensity $\sim 1 \times 10^{11}$ particles per bunch, rms bunch length 40 cm, rms energy spread of 1.2×10^{-4} . Thus, the bunches are stable against fast microwave growth even if the impedance per harmonic is $Z/n \sim 53 \Omega$. The bunch spectrum has a rms spread of 2500 harmonics which is three to four orders of magnitude below the lowest toroidal resonant harmonic. Thus, these toroidal resonances should not have any effects on the bunch stability.

ACKNOWLEDGEMENT

The author was referred to a similar paper written by R.L. Warnock and P. Morton.⁹ They solved the same problem by dividing the vacuum chamber into two radial sections instead. The author would like to thank Dr. Warnock for some very fruitful discussions on both the physics and mathematics of the problem.

	150 GeV		1 TeV	
	TE	TM	TE	TM
n_a	2.52×10^7	6.78×10^7	9.92×10^6	1.83×10^7
f_a	1.20×10^3 GHz	3.24×10^3 GHz	4.73×10^2 GHz	8.73×10^2 GHz
Q_a	4.80×10^4	1.30×10^5	5.63×10^4	6.74×10^4
$\frac{Z_{sh}}{n}$	$4.41 \times 10^{-5} \Omega$	$2.41 \times 10^{-10} \Omega$	$1.04 \times 10^{-2} \Omega$	$1.43 \times 10^{-3} \Omega$
$\frac{Z_{sh}}{n} \Big _{\text{eff}}$	$2.31 \times 10^{-2} \Omega$	$1.26 \times 10^{-7} \Omega$	1.83Ω	0.387Ω

Table VI: Impedances and positions of the lowest TE and TM toroidal resonant modes for the TEVATRON

REFERENCES

1. L.J. Laslett and W. Lewish, Iowa State Report IS-189, 1960.
2. A. Faltens and L.J. Laslett, Proc. of the 1975 ISABELLE Summer Study, July 14-25, 1975, p.486.
3. K.Y. Ng, Fermilab Report UPC-150 (1981).
4. S. Krinsky and J.M. Wang, Particle Accelerators **17**, 109 (1985).
5. In *Superconducting Super Collider Conceptual Design*, Ed. J.D. Jackson, SSC Internal Report SSC-SR-2020, Section 4.5.4, Sept. 1986.
6. B. Zotter, private communication.
7. K.Y. Ng, unpublished.
8. K.Y. Ng, *Principles of High Energy Hadron Colliders*, Part II, The TEVATRON, Ed. H. Edwards and M. Month, (1988) Chapter 8.
9. R.L. Warnock and P. Morton, SLAC Report SLAC-PUB-4562, 1988; to be published in this same volume of Particle Accelerators.

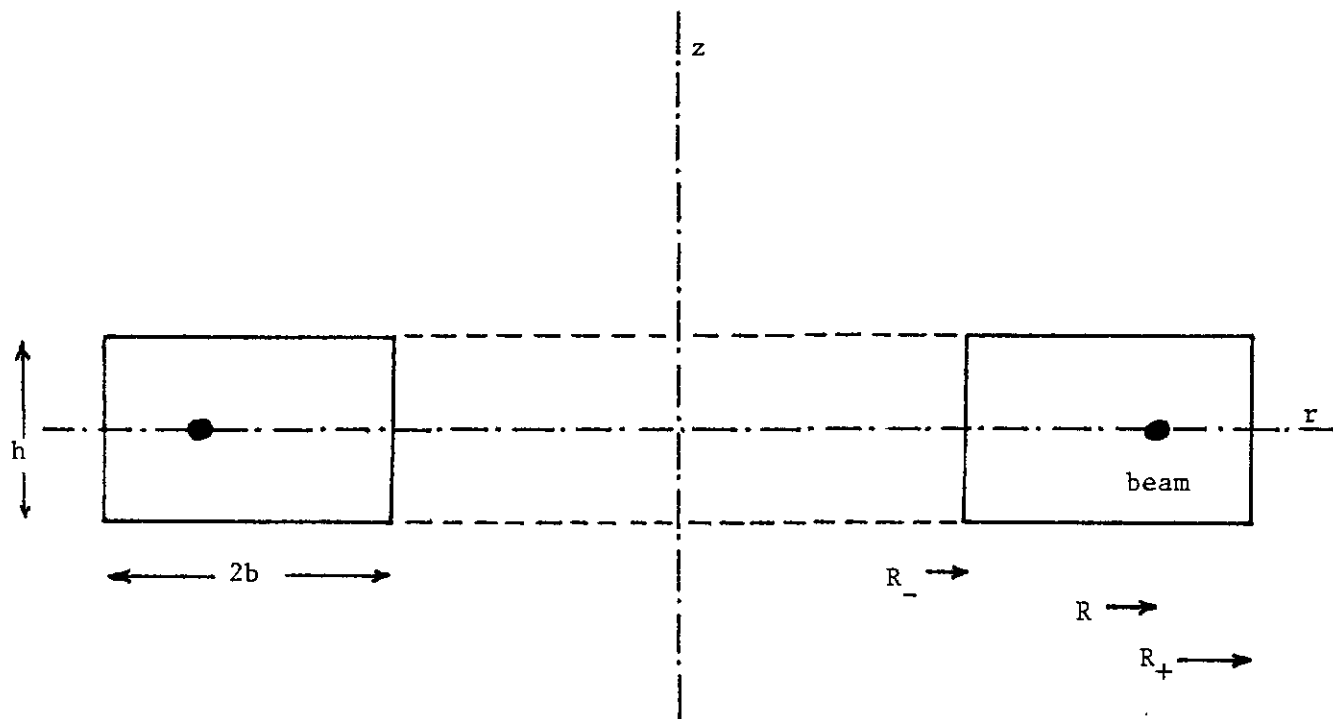


Fig. 1. The toroidal beam pipe with rectangular cross section.

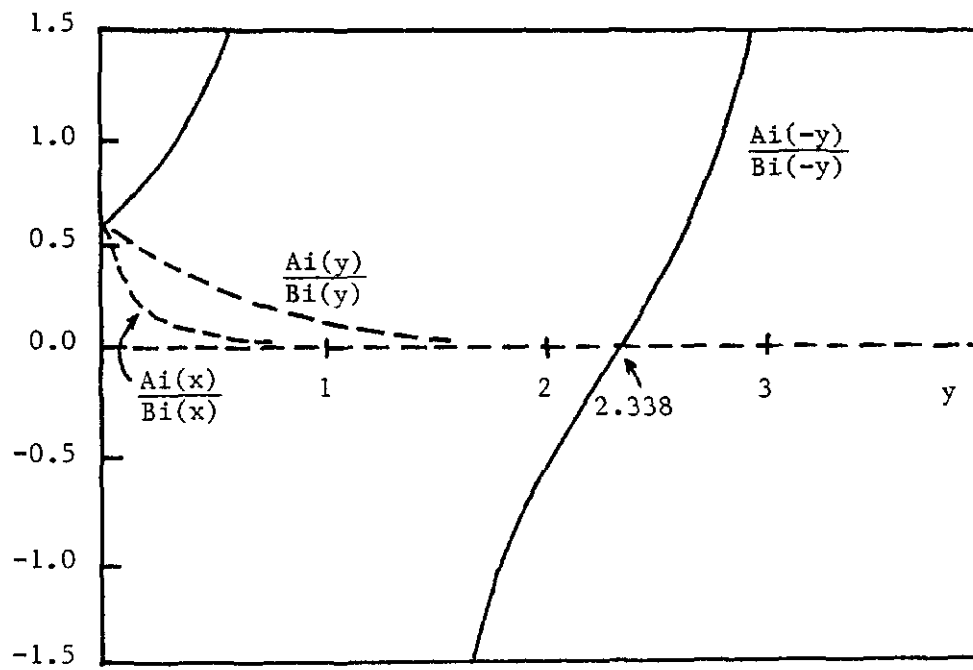
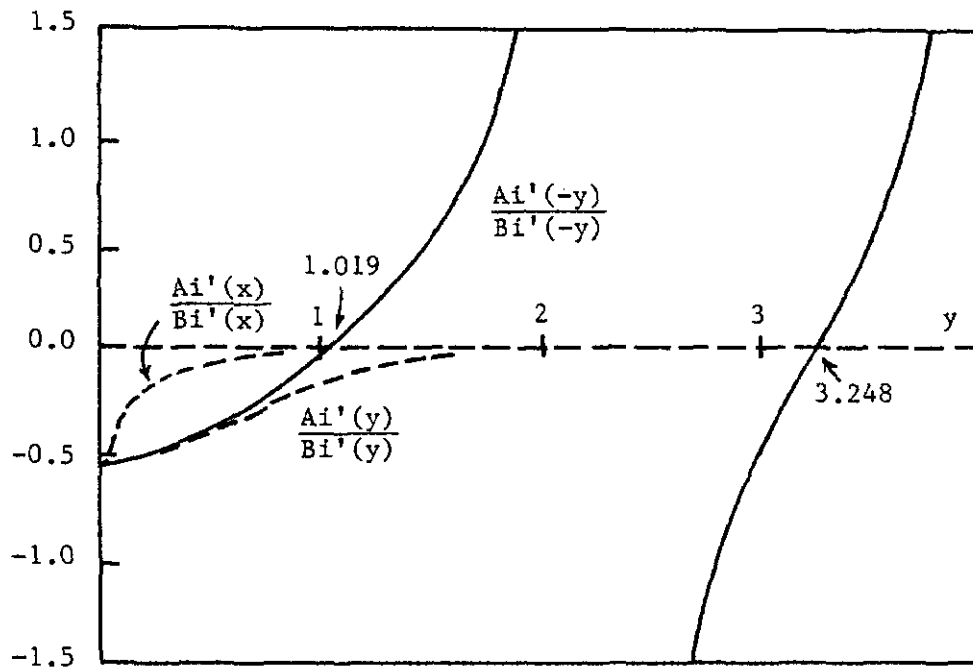


Fig. 2. Plots of Ai/Bi and Ai'/Bi' . x has been taken as $5y$.

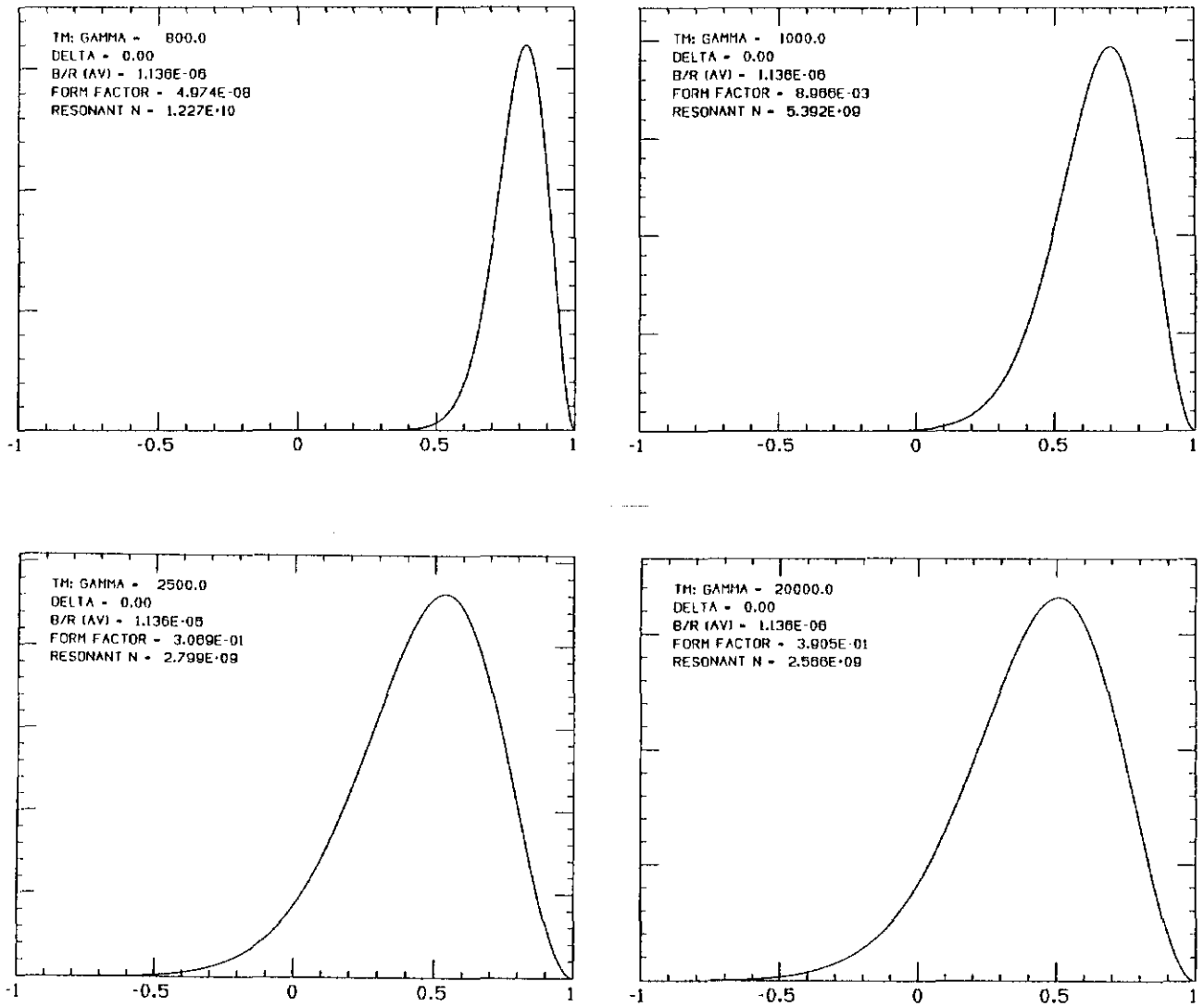


Fig. 3. Plots of the azimuthal electric field $Z(x)$ across the beam pipe for the lowest resonance. On the horizontal axes, $x = -1, 0, 1$ refer to the inner edge, center, outer edge of the beam pipe. The beam is at the pipe center $x = 0$. The vertical scales are arbitrary.

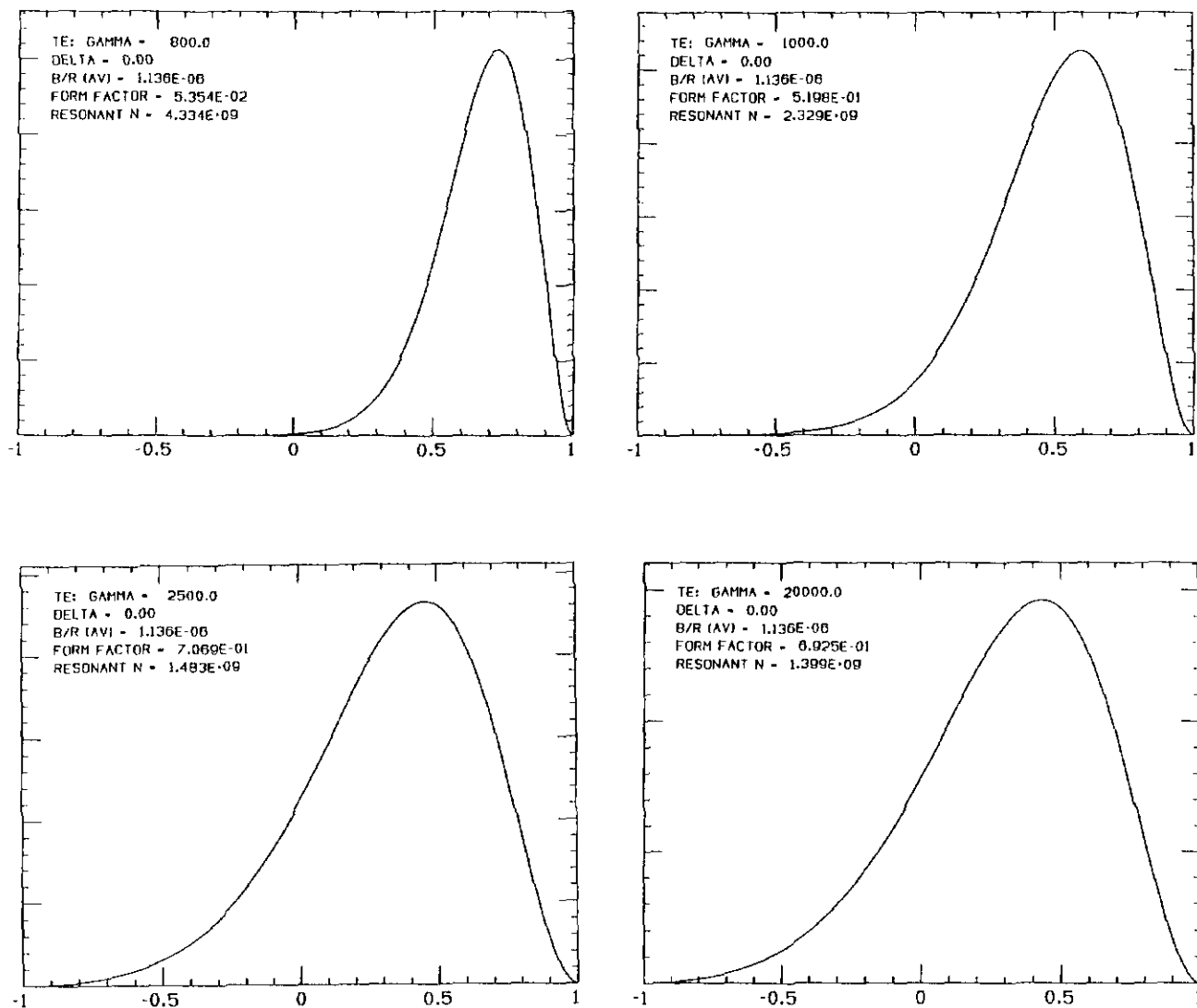


Fig. 4. Plots of the azimuthal electric field $Z'(x)$ across the beam pipe for the lowest resonance. On the horizontal axes, $x = -1, 0, 1$ refer to the inner edge, center, outer edge of the beam pipe. The beam is at the pipe center $x = 0$. The vertical scales are arbitrary.

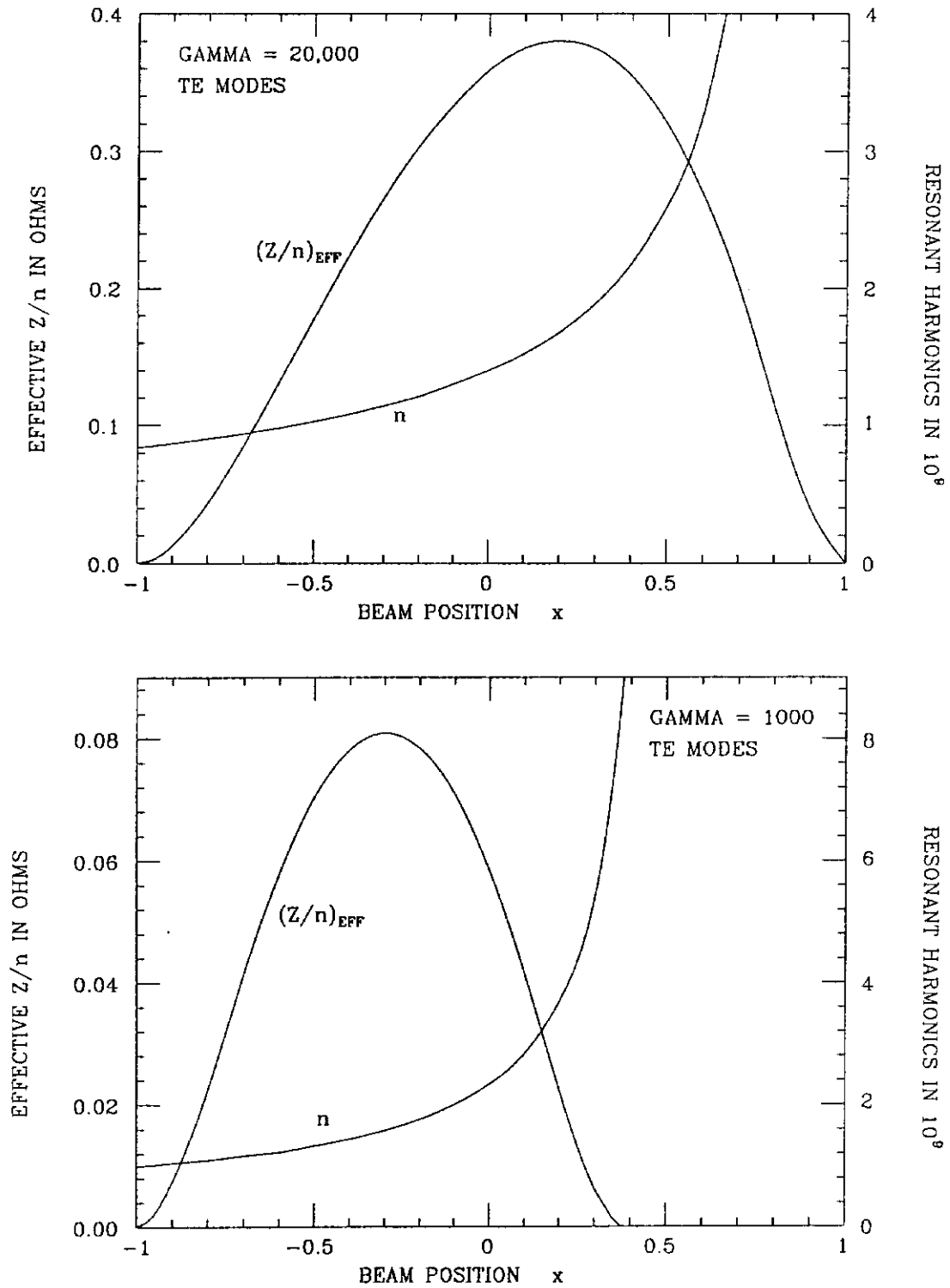


Fig. 5. Effective Z/n and resonant harmonic of the lowest resonance for various beam positions inside a toroidal beam pipe. The beam positions $x = -1, 0, 1$ denote the inner edge, center, outer edge of the beam pipe.

GAMMA = 1000.00 RING RADIUS = 13200.95 M REV FREQ = 3.61439E+00 KHZ
 BEAM PIPE: HALF WIDTH = 0.0150 M FULL HEIGHT = 0.0300 M FRACTIONAL BEAM DISPLACEMENT OUTWARD = 0.00
 WALL CONDUCTIVITY = 1.8000E+09 MHO/M

TE MODES:	F-L	K=1	K=2	K=3	K=4	K=5	K=6	K=7

RADIAL MODE I - 1								
HARMONICS	1.43266E+09	2.32915E+09	4.91165E+09	7.49557E+09	1.00585E+10	1.26065E+10	1.51433E+10	1.76716E+10
FREQ (GHZ)	5.17821E+03	8.41847E+03	1.77526E+04	2.70919E+04	3.63553E+04	4.55647E+04	5.47337E+04	6.38721E+04
Q		2.97143E+06	2.62388E+06	2.44551E+06	2.32836E+06	2.24256E+06	2.17515E+06	2.11993E+06
Z/N (OHM)		0.00000E+00	1.48091E-07	3.70274E-10	1.04812E-12	3.17945E-15	1.00714E-17	3.28575E-20
Z/N_EFF (OHMS)		0.00000E+00	2.77212E-04	1.13490E-06	4.52787E-09	1.78731E-11	7.01167E-14	2.73899E-16
FORM FACTOR		0.00000E+00	2.31328E-02	3.36593E-04	3.24507E-06	2.52181E-08	1.71480E-10	1.06451E-12
RADIAL MODE I - 2								
HARMONICS	8.15595E+09	8.42020E+09	1.00947E+10	1.24042E+10	1.49072E+10	1.74745E+10	2.00652E+10	2.26632E+10
FREQ (GHZ)	2.94788E+04	3.04339E+04	3.64861E+04	4.48336E+04	5.38803E+04	6.31598E+04	7.25235E+04	8.19137E+04
Q		7.64684E+06	7.41938E+06	7.16841E+06	6.95278E+06	6.77121E+06	6.61692E+06	6.48373E+06
Z/N (OHM)		3.15634E-07	1.65873E-08	2.40137E-10	2.10143E-12	1.45059E-14	8.76933E-17	4.87768E-19
Z/N_EFF (OHMS)		3.47556E-04	2.25683E-05	4.15532E-07	4.50558E-09	3.74356E-11	2.65922E-13	1.70494E-15
FORM FACTOR		1.46125E-01	1.63496E-02	5.58523E-04	1.05116E-05	1.40681E-07	1.51292E-09	1.39767E-11
RADIAL MODE I - 3								
HARMONICS	1.47433E+10	1.48904E+10	1.59909E+10	1.78068E+10	1.99973E+10	2.23758E+10	2.48545E+10	2.73886E+10
FREQ (GHZ)	5.32881E+04	5.38196E+04	5.77973E+04	6.43608E+04	7.22783E+04	8.08750E+04	8.98340E+04	9.89933E+04
Q		1.03186E+07	1.01970E+07	1.00157E+07	9.82403E+06	9.64123E+06	9.47404E+06	9.32283E+06
Z/N (OHM)		1.93058E-09	3.17291E-10	1.48160E-11	3.28801E-13	4.70602E-15	5.11472E-17	4.62748E-19

Table II. Toroidal resonant modes for the SSC.

Z/N_EFF (OHMS)	2.78595E-06	4.97576E-07	2.63411E-08	6.69293E-10	1.09220E-11	1.34181E-13	1.35946E-15
FORM FACTOR	6.47772E-03	1.43288E-03	1.04743E-04	3.76935E-06	8.61730E-08	1.45091E-09	1.96703E-11

RADIAL MODE I - 4

HARMONICS	2.13172E+10	2.14175E+10	2.22173E+10	2.36523E+10	2.55132E+10	2.76435E+10	2.99371E+10	3.23371E+10
FREQ (GHZ)	7.70488E+04	7.74114E+04	8.03021E+04	8.54887E+04	9.22147E+04	9.99146E+04	1.08204E+05	1.16879E+05
Q	1.24188E+07	1.23426E+07	1.22148E+07	1.20615E+07	1.19020E+07	1.17441E+07	1.15941E+07	1.15941E+07
Z/N (OHM)	1.48309E-11	4.12863E-12	4.00909E-13	1.81898E-14	4.87305E-16	9.07816E-18	1.30339E-19	1.30339E-19
Z/N_EFF (OHMS)	2.55774E-08	7.43175E-09	7.76306E-10	3.84761E-11	1.13182E-12	2.31413E-14	3.63530E-16	3.63530E-16
FORM FACTOR	1.76970E-04	5.73984E-05	7.23414E-06	4.50006E-07	1.68380E-08	4.37270E-10	8.65721E-12	8.65721E-12

RADIAL MODE I - 5

HARMONICS	2.78873E+10	2.79607E+10	2.85861E+10	2.97517E+10	3.13368E+10	3.32180E+10	3.53110E+10	3.75484E+10
FREQ (GHZ)	1.00796E+05	1.01061E+05	1.03321E+05	1.07534E+05	1.13263E+05	1.20063E+05	1.27628E+05	1.35715E+05
Q	1.42088E+07	1.41564E+07	1.41564E+07	1.40622E+07	1.39418E+07	1.38064E+07	1.36668E+07	1.35277E+07
Z/N (OHM)	1.28667E-13	4.80190E-14	7.48673E-15	5.75640E-16	2.58282E-17	7.69835E-19	1.68700E-20	1.68700E-20
Z/N_EFF (OHMS)	2.53197E-10	9.69650E-11	1.58399E-11	1.29386E-12	6.21424E-14	1.98903E-15	4.68255E-17	4.68255E-17
FORM FACTOR	3.89795E-06	1.59519E-06	2.93779E-07	2.80403E-08	1.60414E-09	6.16741E-11	1.74578E-12	1.74578E-12

Table II (continued)

TM MODES:	F-L	K=1	K=2	K=3	K=4	K=5	K=6	K=7
RADIAL MODE I - 1								
HARMONICS	4.98087E+09	5.39204E+09	7.51057E+09	1.00318E+10	1.26205E+10	1.52195E+10	1.78157E+10	2.04063E+10
FREQ (GHZ)	1.80028E+04	1.94889E+04	2.71462E+04	3.62590E+04	4.56153E+04	5.50093E+04	6.43931E+04	7.37565E+04
Q		5.58214E+06	6.58812E+06	7.61403E+06	8.54008E+06	9.37832E+06	1.01467E+07	1.08594E+07
Z/N (OHM)		2.07449E-07	1.81277E-08	2.10005E-10	1.49768E-12	8.78077E-15	4.64722E-17	2.31190E-19
Z/N_EFF (OHMS)		2.00384E-04	2.06659E-05	2.76691E-07	2.21326E-09	1.42498E-11	8.15962E-14	4.34438E-16
FORM FACTOR		8.96633E-03	2.77667E-04	3.18925E-06	2.59152E-08	1.77019E-10	1.08840E-12	6.23490E-15
RADIAL MODE I - 2								
HARMONICS	1.15149E+10	1.17043E+10	1.30365E+10	1.50872E+10	1.74418E+10	1.99269E+10	2.24735E+10	2.50491E+10
FREQ (GHZ)	4.16195E+04	4.23040E+04	4.71190E+04	5.45309E+04	6.30414E+04	7.20235E+04	8.12279E+04	9.05373E+04
Q		8.22428E+06	8.67970E+06	9.33745E+06	1.00397E+07	1.07311E+07	1.13962E+07	1.20315E+07
Z/N (OHM)		2.58956E-10	2.00503E-10	1.18978E-11	2.59304E-13	3.43988E-15	3.43435E-17	2.86472E-19
Z/N_EFF (OHMS)		3.68531E-07	3.01145E-07	1.92241E-08	4.50485E-10	6.38760E-12	6.77260E-14	5.96422E-16
FORM FACTOR		1.68658E-04	2.11597E-05	7.53742E-07	1.39235E-08	1.78100E-10	1.81331E-12	1.58320E-14
RADIAL MODE I - 3								
HARMONICS	1.80708E+10	1.81909E+10	1.91175E+10	2.07232E+10	2.27425E+10	2.49987E+10	2.73899E+10	2.98612E+10
FREQ (GHZ)	6.53151E+04	6.57489E+04	6.90982E+04	7.49018E+04	8.22004E+04	9.03551E+04	9.89979E+04	1.07930E+05
Q		1.02530E+07	1.05109E+07	1.09434E+07	1.14642E+07	1.20194E+07	1.25811E+07	1.31364E+07
Z/N (OHM)		7.86544E-13	1.43191E-12	2.39221E-13	1.28291E-14	3.54483E-16	6.45415E-18	8.88431E-20
Z/N_EFF (OHMS)		1.39548E-09	2.60439E-09	4.53005E-10	2.54503E-11	7.37274E-13	1.40511E-14	2.01954E-16
FORM FACTOR		2.39760E-06	5.77100E-07	4.60286E-08	1.74384E-09	4.05873E-11	6.81067E-13	9.08195E-15
RADIAL MODE I - 4								

Table II (continued)

HARMONICS	2.46319E+10	2.47171E+10	2.54197E+10	2.67070E+10	2.84198E+10	3.04232E+10	3.26145E+10	3.49345E+10
FREQ (GHZ)	8.90295E+04	8.93373E+04	9.18766E+04	9.65296E+04	1.02720E+05	1.09961E+05	1.17882E+05	1.26267E+05
Q		1.19515E+07	1.21202E+07	1.24233E+07	1.28155E+07	1.32595E+07	1.37287E+07	1.42086E+07
Z/N (OHM)		3.58785E-15	1.00068E-14	3.17406E-15	3.32288E-16	1.69418E-17	5.28932E-19	1.16246E-20
Z/N_EFF (OHMS)		7.42008E-12	2.09872E-11	6.82342E-12	7.36887E-13	3.88720E-14	1.25655E-15	2.85811E-17
FORM FACTOR		3.19812E-08	1.09324E-08	1.48399E-09	9.85286E-11	3.85710E-12	1.02830E-13	2.05803E-15

RADIAL MODE I - 5

** ABNORMAL EXIT from NAG Library routine s17AGF: IFAIL = 1
** NAG hard failure - execution terminated

GAMMA = 20000.00 RING RADIUS = 13200.95 M REV FREQ = 3.61439E+00 KHZ
 BEAM PIPE: HALF WIDTH = 0.0150 M FULL HEIGHT = 0.0300 M FRACTIONAL BEAM DISPLACEMENT OUTWARD = 0.00
 WALL CONDUCTIVITY = 1.8000E+09 MHO/M

TE MODES:	F-1	K-1	K-2	K-3	K-4	K-5	K-6	K-7

RADIAL MODE I - 1								
HARMONICS	6.01321E+08	1.39855E+09	3.33573E+09	5.24814E+09	7.14524E+09	9.03267E+09	1.09137E+10	1.27898E+10
FREQ (GHZ)	2.17341E+03	5.05490E+03	1.20566E+04	1.89688E+04	2.58257E+04	3.26476E+04	3.94462E+04	4.62273E+04
Q		3.25073E+06	2.79887E+06	2.59524E+06	2.46527E+06	2.37058E+06	2.29713E+06	2.23725E+06
Z/N (OHM)		8.35580E-04	6.26046E-06	6.73846E-08	8.29538E-10	1.09123E-11	1.49357E-13	2.09702E-15
Z/N_EFF (OHMS)		3.59488E-01	7.46130E-03	1.36266E-04	2.40430E-06	4.15795E-08	7.09593E-10	1.19881E-11
FORM FACTOR		6.92544E-01	1.95038E-01	1.38720E-02	6.17691E-04	2.15804E-05	6.49610E-07	1.76634E-08
RADIAL MODE I - 2								
HARMONICS	3.42324E+09	3.75390E+09	5.38761E+09	7.29068E+09	9.23230E+09	1.11780E+10	1.31204E+10	1.50567E+10
FREQ (GHZ)	1.23729E+04	1.35681E+04	1.94729E+04	2.63514E+04	3.33692E+04	4.04017E+04	4.74224E+04	5.44209E+04
Q		8.74926E+06	8.23768E+06	7.83317E+06	7.53040E+06	7.29392E+06	7.10240E+06	6.94059E+06
Z/N (OHM)		2.87492E-04	4.00388E-05	2.11336E-06	7.68428E-08	2.32094E-09	6.27909E-11	1.57492E-12
Z/N_EFF (OHMS)		1.23349E-01	2.61862E-02	1.96699E-03	9.42096E-05	3.55686E-06	1.15995E-07	3.41658E-09
FORM FACTOR		4.59536E+00	2.88399E+00	5.36835E-01	5.22105E-02	3.49857E-03	1.84509E-04	8.21326E-06
RADIAL MODE I - 3								
HARMONICS	6.18809E+09	6.38346E+09	7.62733E+09	9.35102E+09	1.12213E+10	1.31421E+10	1.50811E+10	1.70260E+10
FREQ (GHZ)	2.23662E+04	2.30723E+04	2.75682E+04	3.37983E+04	4.05582E+04	4.75006E+04	5.45090E+04	6.15389E+04
Q		1.18833E+07	1.15363E+07	1.11513E+07	1.08175E+07	1.05366E+07	1.02976E+07	1.00911E+07
Z/N (OHM)		1.14971E-04	4.55818E-05	6.68743E-06	5.40472E-07	3.09007E-08	1.41833E-09	5.59864E-11

Table II (continued)

Z/N_EFF (OHMS)	6.17600E-02	3.01369E-02	5.60779E-03	5.60646E-04	3.85417E-05	2.07719E-06	9.44626E-08
FORM FACTOR	1.13138E+01	9.41784E+00	3.22925E+00	5.57895E-01	6.16108E-02	5.01773E-03	3.28348E-04

RADIAL MODE I - 4

HARMONICS	8.94732E+09	9.08394E+09	1.00543E+10	1.15649E+10	1.33118E+10	1.51626E+10	1.70634E+10	1.89894E+10
FREQ (GHZ)	3.23391E+04	3.28330E+04	3.63402E+04	4.18002E+04	4.81143E+04	5.48036E+04	6.16737E+04	6.86353E+04
Q	1.43272E+07	1.40870E+07	1.37623E+07	1.34436E+07	1.31543E+07	1.28979E+07	1.26712E+07	1.26712E+07
Z/N (OHM)	6.09843E-05	3.69501E-05	1.03529E-05	1.54417E-06	1.49986E-07	1.08719E-08	6.40113E-10	
Z/N_EFF (OHMS)	3.86662E-02	2.63724E-02	8.69984E-03	1.52904E-03	1.72885E-04	1.43830E-05	9.59295E-07	
FORM FACTOR	2.04122E+01	1.88773E+01	9.47704E+00	2.54019E+00	4.24435E-01	5.03243E-02	4.62617E-03	

RADIAL MODE I - 5

HARMONICS	1.17049E+10	1.18084E+10	1.25935E+10	1.39084E+10	1.55140E+10	1.72721E+10	1.91114E+10	2.09964E+10
FREQ (GHZ)	4.23062E+04	4.26803E+04	4.55179E+04	5.02706E+04	5.60736E+04	6.24281E+04	6.90762E+04	7.58891E+04
Q	1.64037E+07	1.62290E+07	1.59622E+07	1.56744E+07	1.53973E+07	1.51400E+07	1.49044E+07	1.49044E+07
Z/N (OHM)	3.78750E-05	2.79628E-05	1.17145E-05	2.75998E-06	4.14468E-07	4.45851E-08	3.73855E-09	
Z/N_EFF (OHMS)	2.72647E-02	2.16988E-02	1.02072E-02	2.73174E-03	4.64935E-04	5.62803E-05	5.26662E-06	
FORM FACTOR	3.16163E+01	3.05218E+01	1.93409E+01	7.18360E+00	1.68717E+00	2.76675E-01	3.43319E-02	

RADIAL MODE I - 6

HARMONICS	1.44617E+10	1.45454E+10	1.51997E+10	1.63511E+10	1.78165E+10	1.94683E+10	2.12319E+10	2.30626E+10
FREQ (GHZ)	5.22703E+04	5.25727E+04	5.49377E+04	5.90992E+04	6.43959E+04	7.03660E+04	7.67406E+04	8.33574E+04
Q	1.82435E+07	1.81098E+07	1.78913E+07	1.76373E+07	1.73780E+07	1.71291E+07	1.68946E+07	1.68946E+07
Z/N (OHM)	2.58981E-05	2.12116E-05	1.14540E-05	3.77640E-06	8.05580E-07	1.21352E-07	1.39163E-08	
Z/N_EFF (OHMS)	2.06483E-02	1.78031E-02	1.04679E-02	3.81477E-03	9.02475E-04	1.50419E-04	1.89970E-05	
FORM FACTOR	4.47500E+01	4.40285E+01	3.22278E+01	1.51939E+01	4.68976E+00	1.01393E+00	1.64114E-01	

Table II (continued)

TM MODES:	F-L	K-1	K-2	K-3	K-4	K-5	K-6	K-7
RADIAL MODE I - 1								
HARMONICS	2.09058E+09	2.56617E+09	4.40072E+09	6.34393E+09	8.28635E+09	1.02199E+10	1.21451E+10	1.40626E+10
FREQ (GHZ)	7.55619E+03	9.27517E+03	1.59059E+04	2.29295E+04	2.99502E+04	3.69386E+04	4.38972E+04	5.08278E+04
Q		3.85095E+06	5.04297E+06	6.05486E+06	6.92000E+06	7.68505E+06	8.37771E+06	9.01483E+06
Z/N (OHM)		1.21502E-04	1.67601E-05	6.42644E-07	1.82474E-08	4.52401E-10	1.03747E-11	2.25563E-13
Z/N_EFF (OHMS)		8.09659E-02	1.46256E-02	6.73325E-04	2.18503E-05	6.01618E-07	1.50401E-08	3.51865E-10
FORM FACTOR		3.90530E-01	3.95308E-02	1.96270E-03	7.24178E-05	2.26289E-06	6.35568E-08	1.65265E-09
RADIAL MODE I - 2								
HARMONICS	4.83307E+09	5.07849E+09	6.49957E+09	8.32098E+09	1.02361E+10	1.21761E+10	1.41219E+10	1.60669E+10
FREQ (GHZ)	1.74686E+04	1.83557E+04	2.34920E+04	3.00753E+04	3.69971E+04	4.40092E+04	5.10422E+04	5.80720E+04
Q		5.41742E+06	6.12868E+06	6.93445E+06	7.69114E+06	8.38839E+06	9.03382E+06	9.63586E+06
Z/N (OHM)		1.09573E-05	1.93669E-05	2.61954E-06	1.80106E-07	8.84888E-09	3.55481E-10	1.24762E-11
Z/N_EFF (OHMS)		1.77713E-02	2.05389E-02	3.14332E-03	2.39701E-04	1.28445E-05	5.55698E-07	2.08028E-08
FORM FACTOR		6.64382E-01	1.78847E-01	2.06759E-02	1.49749E-03	8.17053E-05	3.69171E-06	1.45722E-07
RADIAL MODE I - 3								
HARMONICS	7.58474E+09	7.74498E+09	8.83738E+09	1.04530E+10	1.22648E+10	1.41538E+10	1.60780E+10	1.80159E+10
FREQ (GHZ)	2.74142E+04	2.79934E+04	3.19418E+04	3.77811E+04	4.43298E+04	5.11575E+04	5.81122E+04	6.51164E+04
Q		6.69013E+06	7.14638E+06	7.77220E+06	8.41889E+06	9.04402E+06	9.63919E+06	1.02036E+07
Z/N (OHM)		5.41218E-06	1.33002E-05	4.27719E-06	5.93837E-07	5.17759E-08	3.37237E-09	1.79481E-10
Z/N_EFF (OHMS)		6.26553E-03	1.64474E-02	5.75245E-03	8.65113E-04	8.10289E-05	5.62504E-06	3.16900E-07
FORM FACTOR		8.30831E-01	3.60013E-01	7.50109E-02	9.29718E-03	8.09600E-04	5.51479E-05	3.12964E-06
RADIAL MODE I - 4								

Table II (continued)

HARMONICS	1.03386E+10	1.04565E+10	1.13251E+10	1.27336E+10	1.44099E+10	1.62154E+10	1.80875E+10	1.99944E+10
FREQ (GHZ)	3.73677E+04	3.77938E+04	4.09335E+04	4.60241E+04	5.20830E+04	5.86090E+04	6.53755E+04	7.22675E+04
Q		7.77351E+06	8.08996E+06	8.57826E+06	9.12547E+06	9.68030E+06	1.02238E+07	1.07493E+07
Z/N (OHM)		2.16621E-06	8.21897E-06	4.68683E-06	1.12220E-06	1.58356E-07	1.57011E-08	1.21104E-09
Z/N_EFF (OHMS)		2.91386E-03	1.15057E-02	6.95712E-03	1.77206E-03	2.65261E-04	2.77776E-05	2.25262E-06
FORM FACTOR		9.50863E-01	5.30024E-01	1.63996E-01	3.08858E-02	3.98536E-03	3.87740E-04	3.04101E-05

RADIAL MODE I - 5

HARMONICS	1.30930E+10	1.31861E+10	1.38999E+10	1.51279E+10	1.66620E+10	1.83665E+10	2.01691E+10	2.20281E+10
FREQ (GHZ)	4.73234E+04	4.76596E+04	5.02398E+04	5.46783E+04	6.02231E+04	6.63836E+04	7.28990E+04	7.96181E+04
Q		8.72936E+06	8.96253E+06	9.35006E+06	9.81269E+06	1.03024E+07	1.07961E+07	1.12827E+07
Z/N (OHM)		1.05820E-06	5.11578E-06	4.26748E-06	1.54540E-06	3.24164E-07	4.62520E-08	4.96473E-09
Z/N_EFF (OHMS)		1.59846E-03	7.93401E-03	6.90458E-03	2.62409E-03	5.77900E-04	8.64070E-05	9.69301E-06
FORM FACTOR		1.04603E+00	6.75741E-01	2.72916E-01	7.07065E-02	1.26165E-02	1.67231E-03	1.74982E-04

RADIAL MODE I - 6

HARMONICS	1.58481E+10	1.59238E+10	1.65265E+10	1.76064E+10	1.90050E+10	2.06044E+10	2.23250E+10	2.41246E+10
FREQ (GHZ)	5.72814E+04	5.75550E+04	5.97333E+04	6.36365E+04	6.86915E+04	7.44723E+04	8.06915E+04	8.71959E+04
Q		9.59286E+06	9.77271E+06	1.00870E+07	1.04799E+07	1.09120E+07	1.13585E+07	1.18074E+07
Z/N (OHM)		5.88402E-07	3.30007E-06	3.56676E-06	1.76538E-06	5.11499E-07	9.96091E-08	1.43210E-08
Z/N_EFF (OHMS)		9.76728E-04	5.58071E-03	6.22564E-03	3.20145E-03	9.65827E-04	1.95781E-04	2.92603E-05
FORM FACTOR		1.12567E+00	7.98884E-01	3.87927E-01	1.28011E-01	2.97705E-02	5.13872E-03	6.93853E-04

Table II (continued)